Your thesaurus codes are:
03 (11.05.2; 11.07.1; 11.09.2; 11.19.2; 11.19.6; 11.19.7)

ASTRONOMY AND ASTROPHYSICS
July 5, 2001

Properties of tidally-triggered vertical disk perturbations ⋆

U. Schwarzkopf[1,2,⋆⋆] **and R.-J. Dettmar**[2]

[1] Steward Observatory, University of Arizona, 933 North Cherry Avenue, Tucson, Arizona 85721, USA
[2] Astronomisches Institut, Ruhr-Universität Bochum, Universitätsstraße 150, 44780 Bochum, Germany

Received 15 July 2000 / Accepted 12 April 2001

Abstract. We present a detailed analysis of the properties of warps and tidally-triggered perturbations perpendicular to the plane of 47 interacting/merging edge-on spiral galaxies. The derived parameters are compared with those obtained for a sample of 61 non-interacting edge-on spirals. The entire optical (R-band) sample used for this study was presented in two previous papers. We find that the scale height of disks in the interacting/merging sample is characterized by perturbations on both large ($\simeq$ disk cut-off radius) and short ($\simeq z_0$) scales, with amplitudes of the order of 280 pc and 130 pc on average, respectively. The size of these large (short) -scale instabilities corresponds to 14% (6%) of the mean disk scale height. This is a factor of 2 (1.5) larger than the value found for non-interacting galaxies. A hallmark of nearly all tidally distorted disks is a scale height that increases systematically with radial distance. The frequent occurrence and the significantly larger size of these gradients indicate that disk asymmetries on large scales are a common and persistent phenomenon, while local disturbances and bending instabilities decline on shorter timescales. Nearly all (93%) of the interacting/merging and 45% of the non-interacting galaxies studied are noticeably warped. Warps of interacting/merging galaxies are ≈ 2.5 times larger on average than those observed in the non-interacting sample, with sizes of the order of 340 pc and 140 pc, respectively. This indicates that tidal distortions do considerably contribute to the formation and size of warps. However, they cannot entirely explain the frequent occurrence of warped disks.

Key words: galaxies: evolution – galaxies: general – galaxies: interactions – galaxies: spiral – galaxies: structure – galaxies: statistics

Send offprint requests to: U. Schwarzkopf (schwarz@as.arizona.edu)

⋆ Based on observations obtained at the European Southern Observatory (ESO, La Silla, Chile), Calar Alto Observatory operated by the MPIA (DSAZ, Spain), Lowell Observatory (Flagstaff,AZ, USA), and Hoher List Observatory (Germany).

⋆⋆ Lynen Fellow at Steward Observatory

1. Introduction

The vertical structure of galactic disks seen nearly edge-on and, in particular, the behaviour of the disk scale height with galactocentric distance is a major source of information on disk properties, such as their global and local stability, the secular evolution of their stellar population as well as the vertical heating process. Until recently most observational results indicated that the constancy of the scale height over the whole radial extent is a fundamental property of galactic disks (van der Kruit & Searle 1981a,b, 1982; Wainscoat et al. 1989; Barnaby & Thronson 1992). This result was consistent with the theoretical picture of continuously heated disk stars by massive molecular clouds (Spitzer & Schwarzschild 1951; Binney 1981) and with the assumption that at all times the star formation rate is proportional to the number density of molecular clouds (Fall 1980). Hence, also the vertical velocity dispersion of the disk stars should exponentially decrease with radial distance.

Although the overall constancy of the scale height of galactic disks was confirmed thereafter by several studies in the optical and near-infrared, the derived constancy levels differ significantly from each other. While Shaw & Gilmore (1990) found that the intrinsic variation of the disk scale height along the major axis of a galaxy is typically within 3% of its mean value, de Grijs & van der Kruit (1996) obtained a value between $10\% - 15\%$ for Sc and later type galaxies. Reshetnikov & Combes (1996, 1997) have split their galaxy sample into two subsamples and found a dispersion of 7% for non-interacting galaxies, while the heavily disturbed disks of interacting pairs of galaxies (equal mass) possess a dispersion of 11%. Although this is almost twice compared to non-interacting galaxies, their values are still consistent with the above mentioned level found for normal galaxies by de Grijs & van der Kruit (1996). Furthermore, the results of the latter two studies indicate that there is a correlation between the radial behaviour of the scale height and environment.

At present the existing uncertainties cannot be constrained by statistical studies based on a significantly larger and thus more reliable galaxy sample. Hence the

large differences between individual values make it difficult to give a coherent interpretation. Considering that small variations of the scale height are difficult to measure it may be argued that the observed differences are mainly due to a combination of several biasing effects such as selection criteria, the size of the galaxy sample used, or due to different disk models applied for fitting the scale height. On the other hand, there is some evidence for a physically motivated explanation: as a result of a detailed study of vertical surface brightness profiles of edge-on disk galaxies de Grijs & Peletier (1997) found that the exponential scale height increases with distance along the major axis. The effect is strongest for early-type galaxies (increase by 50% for $T = -2$), but negligible for the latest-type galaxies ($T = 8$). Therefore, they concluded that this effect might be closely related to the presence of an underlying thick disk, with a scale length larger than that of the thin disk (with the possibility that thick disks were formed by accretion of small satellites or gas clouds).

Another frequently observed feature of vertical distortions are warped and bended disks. Various theories have been proposed to explain the existence of warps, considering either tidal interactions with neighbouring galaxies (e.g. Schwarz 1985; Zaritsky & Rix 1997), gravitational action of the halo on the disk (Sparke 1984; Sparke & Casertano 1988) or interaction with or accretion of extragalactic gas (Binney 1992). Other possible explanations for gentle warps and bended disks are intergalactic magnetic fields (Battaner et al. 1990) self-gravitation (Pfenniger et al. 1994), or discrete oscillations and bending modes (Sellwood 1996).

The results of recently conducted statistical studies (Sanchez-Saavedra et al. 1990; Reshetnikov & Combes 1998a) enable to limit the number of different explanations given for warped disks. They conclude that at least 50% (up to 80% after correction effects) of all observed galaxies exhibit warped distortions. Furthermore, they find a strong positive correlation of observed warps with the environment, suggesting that tidal interactions have a large influence in creating or re-enforcing warped deformations. In spite of selection biases or identification problems (Sanchez-Saavedra et al. 1990) the fraction of galaxies possessing warps, particularly that of non-interacting galaxies, is unexpectedly high.

In two previous papers (Schwarzkopf & Dettmar 2000a,b, hereafter SD I+II) we studied the global properties of disks in 110 edge-on spiral galaxies. The sample was divided into two subsamples of interacting/merging and non-interacting galaxies. We found that galactic disks recently affected by tidal interactions and minor mergers of the order of $M_{\rm sat}/M_{\rm disk} \approx 0.1$ statistically possess a 50% – 60% larger scale height. However, it is still ambiguous whether this thickening is due to a locally increased disk scale height as a result of the vertical perturbations, or caused by global disk thickening. Moreover, the properties of other tidally triggered features in the disks such as "warps" and "flares" have not yet been investigated.

Therefore, we use the galaxy sample described in SD I+II in order to study the scale height of both non-interacting and interacting/merging galaxies in greater detail. The main questions are:

- How constant is the disk scale height of interacting/merging and non-interacting galaxies?
- Is there a systematic dependence of disk thickness with radial distance (scale height gradients)?
- Do the tidally induced disk perturbations possess a typical size and lifetime?
- Are warped disks restricted to interacting/merging galaxies, and what is the typical size of these warps?

In Sect. 2 of this paper the sample and approach will be briefly reviewed. In Sect. 3 we present the results of a detailed analysis of the vertical disk structure for both non-interacting and interacting/merging galaxies. Finally, the results of this paper will be discussed in Sect. 4 and summarized in Sect. 5.

2. Sample and disk fitting procedure

2.1. The sample

The galaxy sample studied in this paper consists of two subsamples of 47 interacting/merging and 61 non-interacting disk galaxies with morphological types ranging from $-1 \leq T \leq 9$. All galaxies of the optical data set (passbands R and r) presented here are nearly edge-on: 85% with inclinations $i \geq 88°$, and 15% with $i \geq 85°$. Since the whole project (Schwarzkopf 1999 and SD I+II) is focused on the influence of interactions and minor mergers on the disk structure of spiral galaxies only merging candidates in the mass range $M_{\rm sat}/M_{\rm disk} \approx 0.05 - 0.2$ were included in the sample (mean ratio 0.08 ± 0.035). Both subsamples were selected in such a way that selection biases, i.e. an uncertain classification of galaxies belonging to the interacting or non-interacting sample, are largely avoided (SD I, Sect. 2). We have also shown that both the distribution of morphological galaxy types and distances are statistically indistinguishable for the two subsamples (Sect. 2 of SD I+II, resp.). A detailed description of the selection criteria, observations, and data reduction as well as a complete list of the parameters of all sample galaxies and their disk components was given in SD I+II.

2.2. Approach

First, the global disk parameters for each individual galaxy in the sample were roughly estimated using the semi-automated disk fitting procedure described in Sect. 4 of SD I. These disk parameters are: inclination angle i, central luminosity density L_0, cut-off radius $R_{\rm max}$, scale

length h, scale height z_0, and one of the 3 possible vertical disk profiles $f(z) \propto$ exp, sech, and sech^2. Since both the scale height and the choice of the optimum vertical disk profile were still subject of further independent investigation, we used the previously derived mean value of the disk scale height as a starting point for the following vertical fitting procedure. The obtained raidal disk parameters were kept fixed. This is a valid approximation since the effects of small ($\approx 10\%$) variations of vertical disk parameters on radial disk profiles are negligible (SDI, Sect. 4). Thus, the only disk parameter that was changed according to the variable scale height was the central luminosity density L_0.

Using these start parameters a fully automatical least-square fitting procedure was applied in order to fit the disk scale height as a function of the galactocentric distance, $z_0(R)$. The fit was performed for all 108 galaxies of the total sample, and for each vertical disk model $f(z)$. Due to their importance for the subsequent analysis of the vertical disk structure the main features of this fitting procedure and its output parameters (listed in Table 4) are described in the following (for an illustration see examples in Figs. 2-4 and 6):

- The scale height was fitted to the vertical disk profiles, starting in a region as close as possible to the galactic plane but outside the strongest dust absorption, out to $\approx 2\,z_0$. The radial fit region covers both sides of the major axis out to the disk cut-off, and outside the bulge-contaminated region. The selection of the fit regions (Table 1) depends on the S/N ratio of the individual image as well as on several other factors (dust, foreground stars, position of companions, warps, etc.).
- The mean disk scale height $(z_0)_{\rm mean}$, given in pc, and its standard deviation $(z_0)_{\rm std}$, given both in pc and in percent of $(z_0)_{\rm mean}$, were estimated. These values (average from both disk sides) are listed in Table 4, columns (4) and (6), respectively.
- A possible gradient (or constancy) of the disk scale height along the major axis, in the following referred to as $(z_0)_{\rm grad}$, was identified by using a 1st order fit (average of both sides) on the radial distribution of disk scale height. Thus the value $(z_0)_{\rm grad}$ is a reliable estimate of the behaviour of disk scale height on large ($\approx R_{\rm max}$) scales (column (5) in Table 4).
- The variations of z_0 around the gradient $(z_0)_{\rm grad}$, i.e. an estimate of vertical disk perturbations on short scales and hereafter $(z_0)_{\rm std1}$, were defined as the standard deviation of the first order fit to the disk scale height: $(z_0)_{\rm std1} = {\rm std}[(z_0)_{\rm grad} - z_0({\rm R})]$. The value $(z_0)_{\rm std1}$ (average of both disk sides) is given in pc and in percent of $(z_0)_{\rm mean}$ (column (7) in Table 4).
- The standard deviation around the position found for the mean galactic plane, named as "Warping" in column (8) of Table 4, was used as an estimate for the mean amplitude of stellar warps. It was calculated using the center of symmetric vertical disk profiles.
- The complete vertical fit, $z_0(R)$, for all galaxies in the sample was performed for each individual luminosity profile $f(z) \propto$ exp, sech, sech^2. The two quantitative best disk models, listed in column (3) of Table 4, were selected using the goodness-of-fit parameter Q of the least-square test, which is given in Table 4, column (9).

Table 1. Regions adopted for fitting the disk scale height z_0. Columns: (1) Sample used for the statistics: total= all galaxies ($n = 108$); non-int.= non-interacting galaxies ($n = 61$); int./merg.= interacting/merging galaxies ($n = 47$); (2) Radial region used for the fit (avg. values, given in units of disk cut-off radius $R_{\rm max}$ and disk scale length h); (3) Vertical region used for the fit (avg. values, given in units of disk scale height z_0).

Sample	Radial region of fit		Vertical region of fit
	$[R_{\rm max}]$	$[h]$	$[z_0]$
(1)	(2)		(3)
total	0.23 – 0.83	0.76 – 2.77	0.11 – 1.81
non-int.	0.24 – 0.82	0.79 – 2.69	0.08 – 1.95
int./merg.	0.21 – 0.83	0.72 – 2.85	0.15 – 1.67

The software used for the fit was designed primarily to characterize the vertical disk structure of a large number of galaxies in a statistically systematical and homogeneous way. Therefore we decided to use mean values and standard deviations as output parameters for quantifying the properties of the disks. This makes the applied method very robust against "outliers". The obtained results (Tables 2 - 4) are thus statistically more reliable than measurements emphasizing individual amplitudes of vertical disk perturbations.

The first part of the paper provides a small sample of spiral galaxies that were found to be "prototypes" for particular disk features. They were included in order to illustrate the behaviour of the scale height. A summary of all measured disk parameters is given in Table 4. The appendix shows the behaviour of disk scale height and mean galactic plane for the complete sample of 108 objects. The variations of disk thickness (upper panels) and galactic plane (lower panels) are drawn to the same scale. The sample of interacting/merging galaxies is shown in Appendix A, and Appendix B contains the non-interacting galaxies. The corresponding catalog of contour maps can be found in Figs. 4 and 5 of SDI, respectively.

3. Results

3.1. The radial behaviour of the disk scale height

The behaviour of the disk scale height as a function of galactocentric distance, $z_0(R)$, is studied for the total

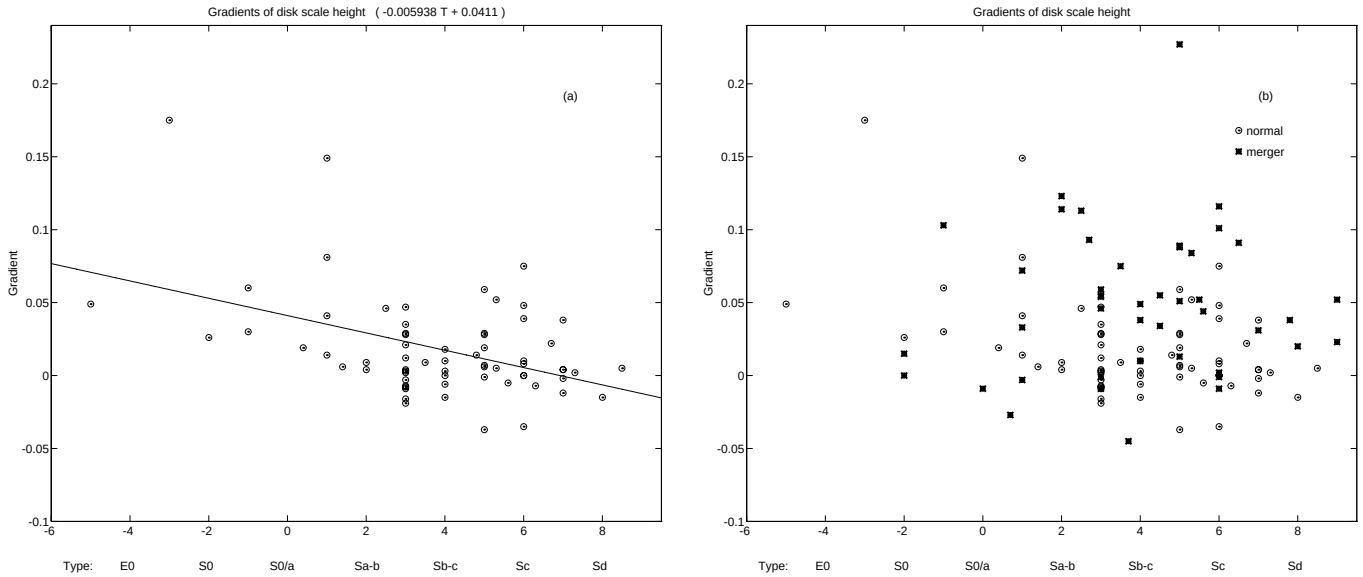

Fig. 1. Gradients $(z_0)_{\rm grad}$ of disk scale height (taken from Table 4, column (5)) versus morphological galaxy type. Shown are **(a)** the sample of non-interacting galaxies, **(b)** both samples of non-interacting and interacting/merging galaxies.

galaxy sample. A short description of the applied fitting procedure and their output parameters was given in Sect. 2. The complete set of parameters obtained from an analysis of the vertical disk structure is listed in Table 4.

In order to derive reliable fit parameters it is important to use similar regions for both the radial and vertical fit, independent of the subsample investigated. As shown in Table 1, the radial and vertical fit regions used for the two galaxy samples are typically between $0.76 - 2.77$ disk scale lengths and $0.11 - 1.81$ scale heights and thus almost identical. These regions nearly cover the whole disk outside the bulge-contaminated region (named as "bulge" in the plots of the disk scale height). All galaxies in the sample are nearly edge-on (Sect. 2), and the vertical profiles were fitted out to ≈ 2 scale heights (Table 1). As a result the influence of dust on the shape of the vertical profiles and thus on the measured scale heights is negligible. This is confirmed by comparable results obtained after fitting $\approx 50\%$ of the sample galaxies in the near-infrared (Table 3 and Sect. 3.3 in SD II). All images used for this study were binned radially by $\approx 2''$ in order to increase the S/N ratio. In order to retain the full vertical resolution no binning was applied in that direction. For the majority of galaxies within a distance of 10 Mpc – 50 Mpc this gives a radial and vertical spatial resolution between 100 pc – 600 pc and 10 pc – 50 pc, respectively. This resolution is sufficient to detect even small deviations and perturbations in the vertical disk structure.

3.1.1. The mean value of the disk scale height

The mean value $(z_0)_{\rm mean}$ of the disk scale height and its error $(z_0)_{\rm std}$, measured for all galaxies of the two subsamples, are listed in columns (4) and (6) of Table 4, respectively. Since many disks show medium or even large gradients in the scale height (i.e. their scale height increases significantly with radial distance, see next section) the obtained errors for the total sample are spread in a wide range around an average value of $(z_0)_{\rm std} \approx 12\%$ (Table 2, column (2)). Within this error the measured scale heights $(z_0)_{\rm mean}$ are consistent with those obtained using an independent, semi-automated fitting procedure (described in Sect. 4 of SD I, values listed in Fig. 5 and Table 5 of SD II). Both methods also independently deliver the same difference between the mean scale height of both subsamples, which was interpreted as tidally-triggered vertical heating in SD II. As a result, disks of interacting/merging galaxies were found systematically $\approx 50\%$ thicker than those of non-interacting galaxies. A detailed discussion of the results and the derived conclusions can be found in SD I+II.

3.1.2. The increase of scale height (gradients)

The behaviour of the scale height over the whole radial extent of the disk, i.e. its gradient $(z_0)_{\rm grad}$, is listed in column (5) of Table 4. In the following we will use the term "gradient" independently whether there is an observed increase or decrease of the scale height ($z_{0\rm grad} \neq 0$) or not ($z_{0\rm grad} = 0$). In Fig. 1 the measured gradients are plotted against the morphological type of the galaxies (both subsamples are shown). Although the correlation is weak, Fig. 1a indicates that the scale height of non-interacting, early-type ($T \leq 2$) galaxies increases towards the outer parts of the disk. While the obtained values are relatively large ($z_{0\rm grad} > 0.04$) almost no gradients were found for non-interacting galaxies with $T \geq 3$.

In order to illustrate the different radial behaviour of disk scale heights Fig. 2 shows, as an example, the results of vertical fits obtained for 4 galaxies of the non-interacting sample with morphological types ranging from $-1.0 \leq T \leq 7.0$. The used disk parameters as well as the corresponding scale height gradients, $(z_0)_{\rm grad}$, are indicated. The reason for the relatively weak correlation with type is the high intrinsic scatter. This scatter is due to a number of disks that show considerably low or high gradients compared to the mean level for galaxies with about the same morphological type.

Although many of the interacting/merging spirals in our sample possess considerable gradients (Fig. 1b) no systematic correlation between these gradients and morphological type was found. The size and substructure of scale height gradients within the sample of interacting/merging galaxies will be investigated in greater detail in the next section, together with an analysis of accompanying environmental effects like disk "warping" and "flaring".

3.1.3. Tidally-triggered vertical disk perturbations

In this section we investigate the typical size of tidally induced vertical perturbations in the disk and compare them with values found for non-interacting galaxies. In order to quantify the perturbations both subsamples of non-interacting and interacting/merging galaxies were compared using the disk parameters $(z_0)_{\rm std}$ and $(z_0)_{\rm std1}$. The approach was described in Sect. 2. Due to their importance for the forthcomming analysis of the vertical disk structure in the following we give a brief interpretation of these parameters (listed in columns (6) and (7) of Table 4).

The standard deviation $(z_0)_{\rm std}$ of the mean scale height characterizes the *sum* of all those vertical variations that are due to both perturbations on short ($\approx z_0$) scales (e.g. "flaring") *and* a possibly systematical trend (scale height gradients). By contrast, the standard deviation $(z_0)_{\rm std1}$ of the first-order fit of the scale height considers a large-scale gradient and only gives an estimate of vertical disk perturbations on short scales. The values $(z_0)_{\rm std}$ and $(z_0)_{\rm std1}$ are listed in columns (2) and (3) of Table 2, respectively (averaged for the total galaxy sample and for both subsamples).

According to Table 2 the obtained results can be summarized as follows: the typical size of vertical disk perturbations in interacting/merging galaxies – including both gradients on large scales as well as perturbations on short scales – is $\approx$ 14% of the mean scale height. The corresponding value found for non-interacting spirals is $\approx$ 10%. In order to compare both values it must be considered that disks of interacting/merging galaxies were found to be systematically thicker by $\approx 50\% - 60\%$ on average (Sect. 3 of SD II and previous section of this paper). Applying this correction the relative size of vertical disk perturbations in interacting/merging and non-interacting galaxies is of the order of 22% and 10%, respectively (normalized to the scale height of non-interacting galaxies). This factor of two is confirmed by the absolute size of 280 pc and 140 pc measured for the perturbations (Table 2, column (2)).

Table 2. Size of vertical disk perturbations and warps. Columns: (1) Galaxy sample used for the statistics: total= all; non-int.= non-interacting; int./merg.= interacting/merging; (2) and (3) Scale of vertical disk perturbations, i.e. (2) sum of (large+short) and (3) short-scale perturbations only, given in percent of mean disk scale height $(z_0)_{\rm mean}$ and in pc (average values, derived from $(z_0)_{\rm std}$ and $(z_0)_{\rm std1}$ in Table 4, resp.); (4) Disk warping, given in percent of $(z_0)_{\rm mean}$ and in pc (average values, derived from column (8) in Table 4).

Sample	Scale of vertical perturbation				Disk	
	large + short		short-scale		Warping	
	[%]	[pc]	[%]	[pc]	[%]	[pc]
(1)	(2)		(3)		(4)	
total	12	210	6	100	14	220
non-int.	10	140	6	80	11	140
int./merg.[a)]	14 (22)	280	6 (9)	130	17 (26)	340

[a)] Values in parenthesis are normalized to the disk thickness of non-int. galaxies, i.e. corrected by a factor of 1.5.

The size of disk perturbations on short scales is, although statistically significant, considerably smaller and typically of the order of 130 pc and 80 pc for the sample of interacting/merging and non-interacting galaxies, respectively. This fact is likely due to a combination of two different properties of such perturbations on short scales, namely their transient character and a systematically smaller amplitude of the induced distortions itself. As a result of the first of these effects the amplitude of the perturbations, and thus the velocity dispersion of disk stars within this region, would subside. Since the size of the affected region ($\approx$kpc) is small compared to the radial extend of the disk the vertical motion excess could be absorbed by neighbouring disk stars. This would contribute to an overall increase of vertical velocity dispersion and thus to a larger value for the scale height (SD II). However, the existing measurements (Table 2, columns (2) and (3)) do not allow us to disentangle the individual effects nor to draw conclusions about their significance. We therefore infer that tidally-triggered, vertical disk asymmetries on large ($\approx R_{\rm max}$) scales are a common and persistent phenomenon, while perturbations on small ($\approx z_0$) scales are systematically smaller and decline on shorter timescales.

3.1.4. Properties of tidally distorted disks

In addition to the statistical differences found between both galaxy samples we also studied the properties of vertical, tidally-triggered disk perturbations in individual galaxies. This also allows a better illustration of some

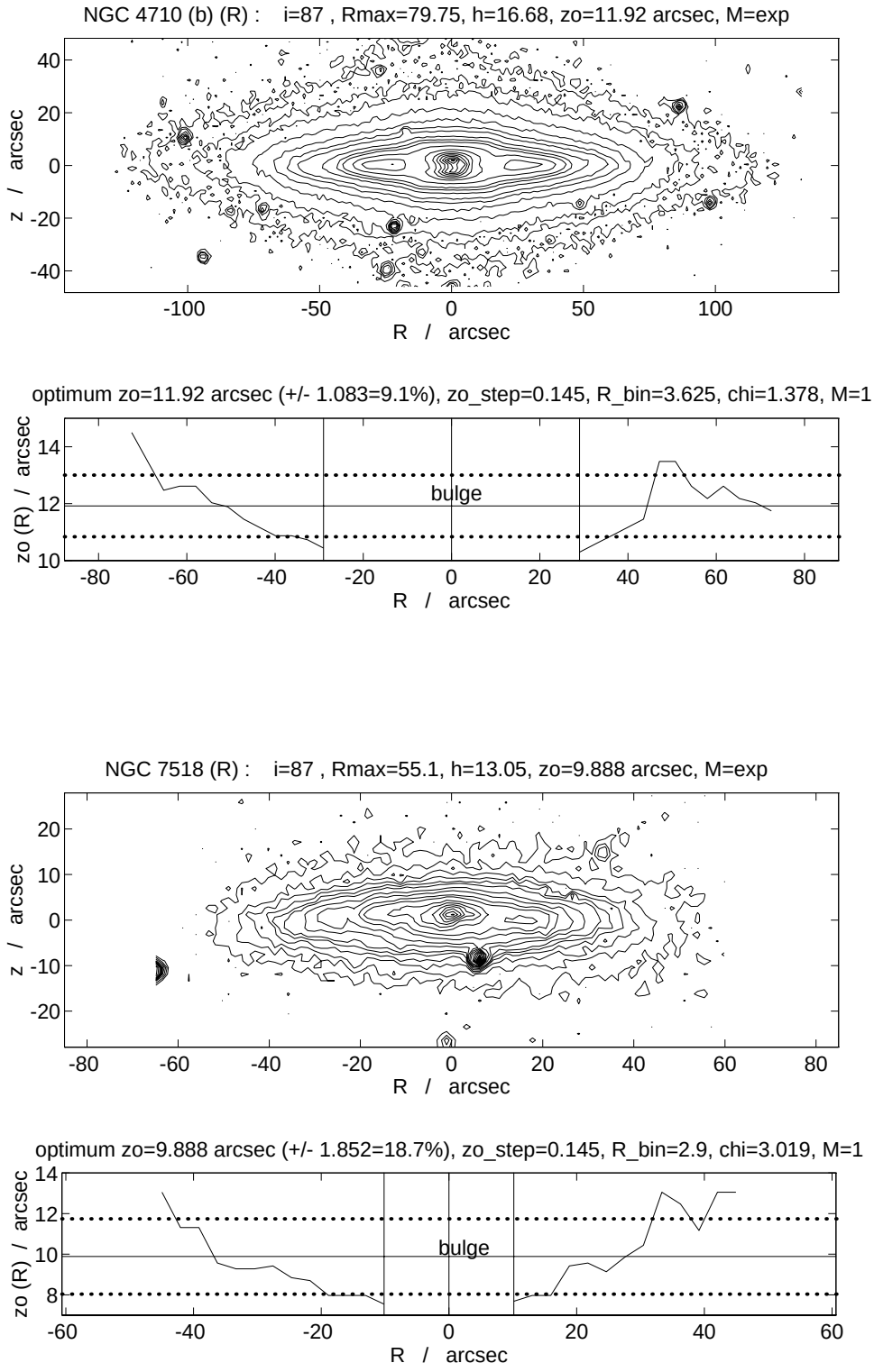

Fig. 2. Examples of non-interacting galaxies with morphological types between $-1 \leq T \leq 6$ showing different levels of variation in their scale height (corresponding lower panels). The galaxies, their type and the measured scale height gradients are: NGC 4710, $T = -1.0$, $(z_0)_{\rm grad} = 0.06 \pm 0.009$ and NGC 7518, $T = 1.0$, $(z_0)_{\rm grad} = 0.149 \pm 0.008$.

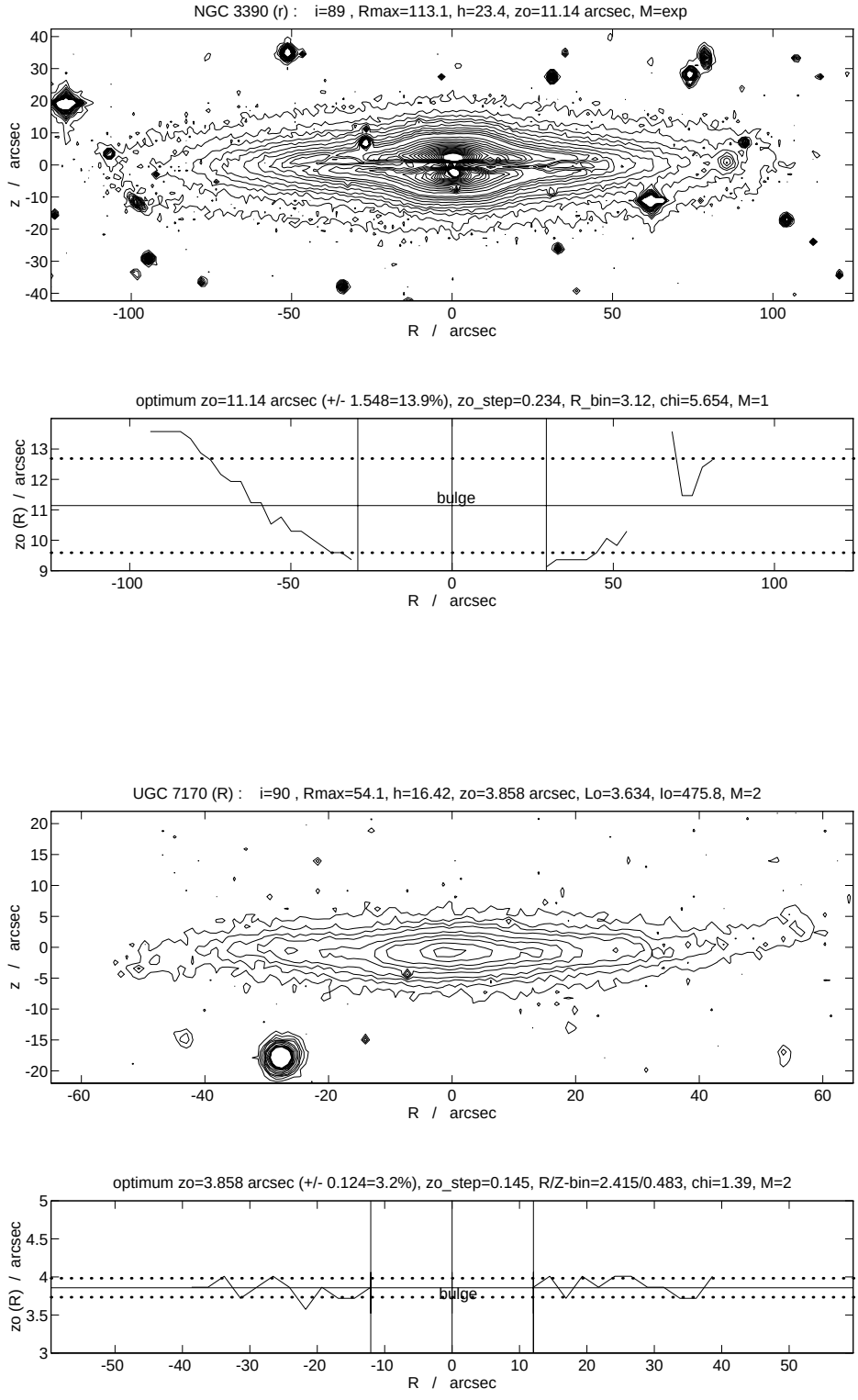

Fig. 2. (continued) NGC 3390, $T = 3.0$, $(z_0)_{\rm grad} = 0.03 \pm 0.009$ and UGC 7170, $T = 6.0$, $(z_0)_{\rm grad} = 0 \pm 0.003$.

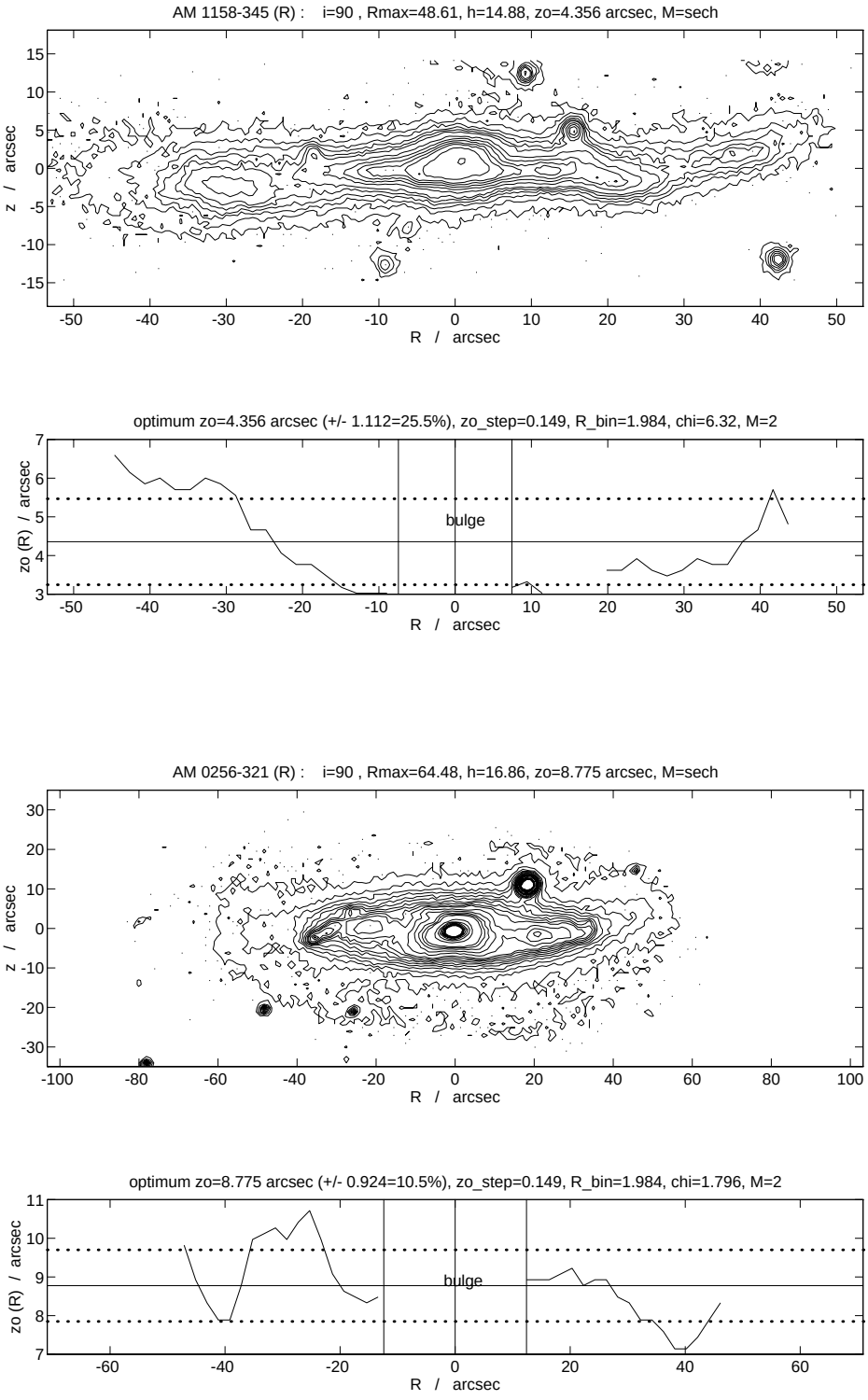

Fig. 3. Two examples of galaxies seen during a phase of an ongoing minor merger. The small companion and/or material of debris are still visible. The corresponding lower panels show variations of the scale height over the whole radial extent of the disk: a large scale height gradient for AM 1158-345 (above) and variations on short scales for AM 0256-321 (below).

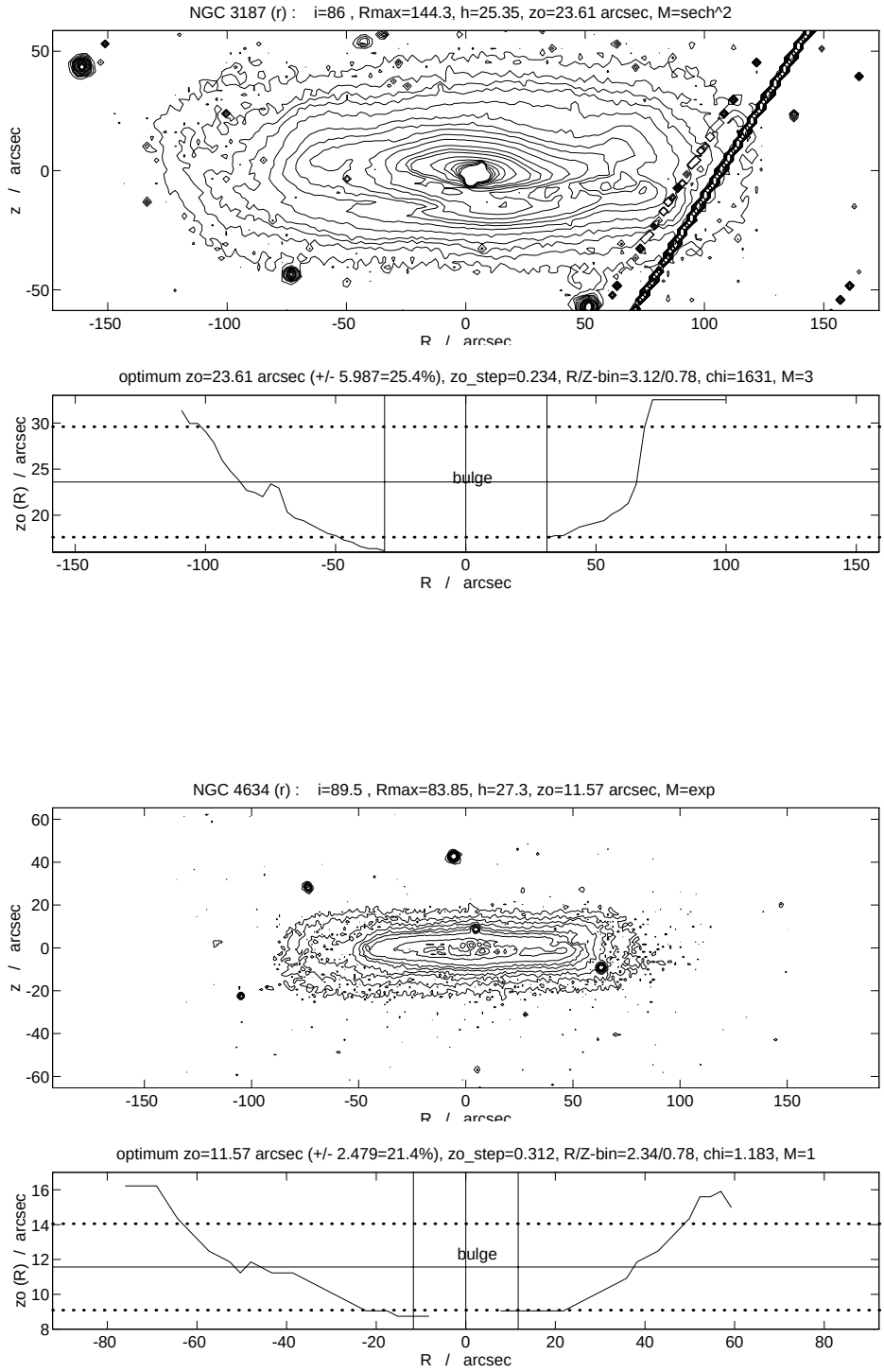

Fig. 4. Two examples of late-type ($T = 5$ and 6) edge-on spirals possessing a considerable increase of scale height with radial distance and hence large scale height gradients (between 0.12 and 0.23). The outer parts of their disks show "fringed" isophotes. Both galaxies are members of compact groups and have been affected by tidal interactions in the past.

of the previously obtained results. We therefore selected 4 galaxies in different stages of the interacting/merging process that clearly display some of the above mentioned properties of galactic disks. The upper panels of Figs. 3 and 4 show these galaxies together with the adopted disk parameters. The corresponding lower panels display the radial behaviour of their scale height.

Figure 3 shows two galaxies in a transient phase of the merging process, accreting a low-mass satellite. While the small companion and its tidal debris are still clearly visible (left part of the disk in both images) the measured radial behaviour of scale height shows significant variations on short scales. The amplitude of these variations is ≈ 1.5 times the mean scale height of the corresponding object. In the case of AM 1158-345 the lower panel clearly shows that the scale height increases substantially towards the outer parts of the disk while showing significant perturbations on small scales at the same time. The first of these two effects is responsible for the large scale height gradient of the order of $(z_0)_{\rm grad} \approx 0.05$ (depending on the vertical disk model used for the fit; for comparison see Fig. 1). It also causes the large deviation of $\approx 25\% - 30\%$ of $(z_0)_{\rm mean}$ that was found for the scale height of this disk. The disk of AM 0256-321 shows perturbations on short scales with large amplitudes of the order of 10%. There is no evidence of a significant gradient of the scale height. This behaviour was found to be typical for those galaxy disks observed in a transition phase of a still ongoing interacting/merging process.

Figure 4 shows two examples of late-type ($T = 5, 6$) edge-on spirals that are, suggested by their location in compact groups of galaxies (Verdes-Montenegro et al. 1998; Zepf 1993) and by the typical features detected in their isophotes, in a more progressed phase of the interaction/merging process. Although there is evidence that these galaxies were strongly affected by such events in the recent past it is not clear whether their disk properties do result from accreting a small companion or from tidal interactions without a merger. However, the behaviour of the scale height of these disks is characteristic for many galaxies in the interacting/merging sample: they show substantial scale height gradients between 0.1 and 0.25, caused by a $1.5 - 2.5$ times larger scale height in a region between 0.5 and 4 disk scale lengths (exceeding slightly the upper limit of the fit region used in the right part of the NGC 3187-panel). Furthermore, the outer isophotes of NGC 3187 and NGC 4634 both show significantly "fringed" disks. The deviations $(z_0)_{\rm std}$ from their mean scale heights were found to be between 22% and 26%. Considering their morphological types ($T = 5 - 6$) and the derived ratio between radial and vertical scale parameters ($1 \leq h/z_0 \leq 2$) their disks are ≈ 4 times thicker than those of typical non-interacting galaxies of the same type (Figs. 6 and 7 in SD II).

Despite the described variety of the radial behaviour of the disk scale height within the sample of interacting/merging galaxies the obtained measurements suggest that perturbations on large scales (i.e. gradients) are a widely common feature, while perturbations on small scales seem to be typical only during an ongoing phase of accretion or interaction (Table 2, columns (2) and (3)). Furthermore, our data indicate that galaxy disks possessing a considerable scale height gradient do also show a smoother trend of the measured scale height with radial distance, i.e. a smaller level of short-scale perturbations. The detection of features like scale height gradients and perturbations on both short and large scales as described in this section is consistent with results of N-body simulations analyzing the stability of galaxy disks as a result of minor mergers (Tóth & Ostriker 1992; Mihos et al. 1995) and with studies of the stability of galactic disks in general (Griv & Peter 1996c).

3.2. Size, type, and frequency of stellar warps

The majority of galaxies in our interacting/merging sample as well as some of the non-interacting galaxies show substantial geometrical distortions. Apart from vertical perturbations studied in the previous section the most frequently observed kind of distortions are variations of the geometrical center of vertical disk profiles around a mean galactic plane, i.e. "warps". In the following we investigate their relative and absolute sizes, their types and the frequency of occurrence for both galaxy samples. The method used for quantifying warped disks was described in Sect. 2.

Due to the sensitivity of the applied fitting procedure we are able to detect vertical deviations from the mean galactic plane of the order of 10 pc – 50 pc, depending on the distance of galaxies (Sect. 3.1). In order to evaluate the influence of dust extinction, misaligned warps, and the appearance of spiral structures on the detection of warps we refer to a series of studies performed by Reshetnikov & Combes (1998a, 1998b), in which these effects were statistically studied in great detail. According to their results, in particular the simulations presented in section 4 and Fig. 10 (same section) of the first paper, the probability of false detections of S-shaped warps is around 30% for disks with inclinations $i \approx 85°$, and drops to 0% for $i \approx 90°$. The simulations were performed for 405 flat model galaxies with a $B/D = 0.3 - 0.5$, axis ratios $a/b > 7$ (average $a/b \approx 9.1$), and with a nice contrasted spiral structure (the latter two properties both overestimate the simulated projection effects with respect to the sample studied in this paper). According to Fig. 10 in Reshetnikov & Combes (1998a) we therefore estimate that the percentage of false S (U)-shaped warps due to projection effects is smaller than 10% (5%) for our highly inclined (85% $\geq 88°$ and 15% $\geq 85°$) galaxy sample. This statistical uncertainty is smaller than the error introduced by the applied visual classification of warp types ($\approx 10\% - 15\%$) and does there-

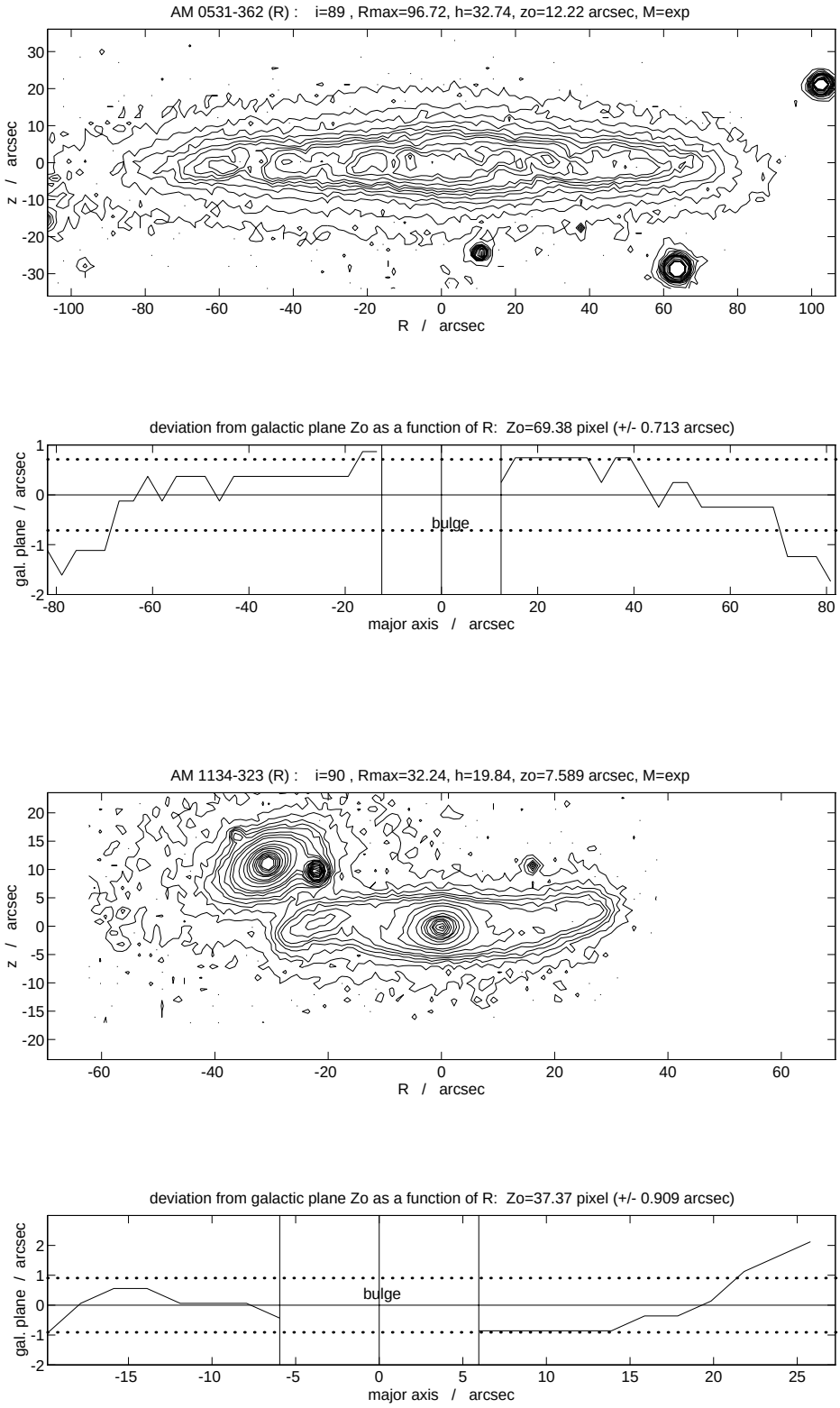

Fig. 6. Examples of different types of warps, shown together with the corresponding variations around the mean galactic plane: U-shaped warp (upper two panels) and S-shaped warp (lower two panels).

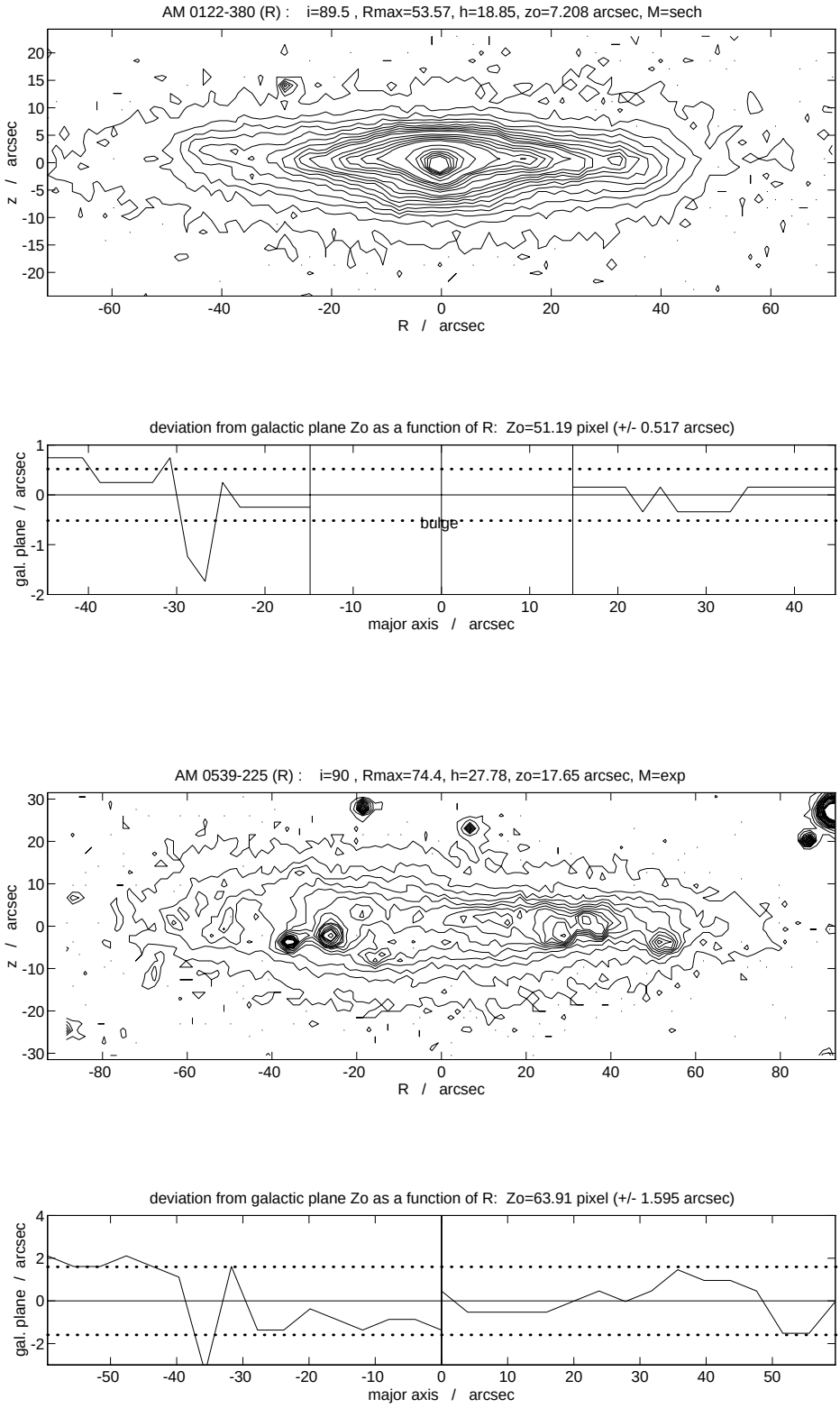

Fig. 6. (continued) *One – side* warp (upper two panels) and *Irr* warp (lower two panels).

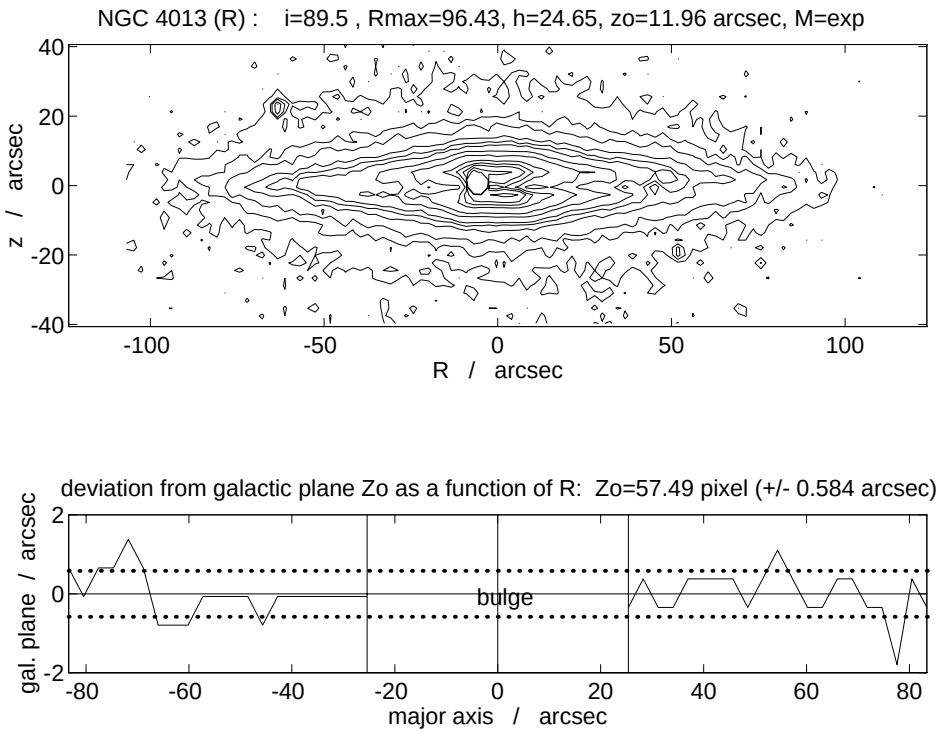

Fig. 6. (continued) Galaxy disk without significant warps.

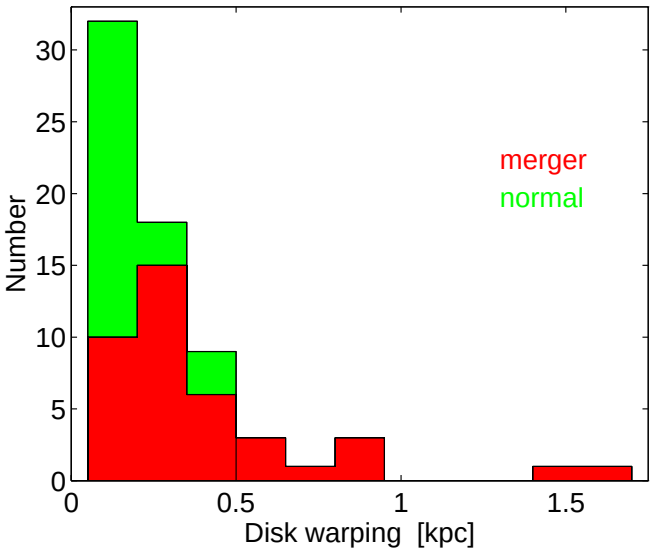

Fig. 5. The size of warps in galactic disks (average values), shown for the sample of non-interacting and interacting/merging galaxies.

Table 3. Types and frequency of optical stellar warps. Columns: (1) Galaxy sample used for the statistics: total= all; non-int.= non-interacting; int./merg.= interacting/merging; (2) Fraction of galaxies (in percent of the investigated sample) with warped disks, for explanation of types see Sect. 3.2.

Sample	Frequency of warp type [%]				
	U-shaped[a)]	S-shaped[a)]	One-side	Irr	None
(1)	(2)				
total	19	24	20	3	34
non-int.	8	19	16	2	55
int./merg.	33	31	25	4	7

[a)] Types according to Reshetnikov & Combes (1998a).

fore not affect the results and conclusions of this study (Table 3).

One of the most unexpected results derived from the standard deviation around the mean galactic plane (named as "Warping" in column (8) of Table 4) was that *all* galaxy disks investigated are warped on some level. However, clear differences in the size of warps between both subsamples can be seen (Fig. 5 and Table 2). Figure 5 shows the distribution of absolute sizes of warps for both subsamples of non-interacting and interacting/merging galaxies. Most of the non-interacting galaxies possess disks with warps that have amplitudes around 140 pc on average, corresponding to $\approx$ 11% of the mean scale

height of these disks. In contrast the majority of interacting/merging galaxies shows considerably warped disks with amplitudes up to $\approx$ 1 kpc, and with an average size of 340 pc. This value corresponds to $\approx 17\%$ of their mean scale height and $\approx 26\%$ of the scale height of non-interacting galaxies (column (4) in Table 2).

In addition to the size of warps their different types and their frequency of occurrence were investigated. In order to classify the types we visually inspected the results of the above described vertical fitting procedure, i.e. the behaviour of vertical variations around the mean galactic plane along the major axis of the disk (shown in the corresponding lower panels of Fig. 6). For our classification we distinguished four different types of warps (the plots in Fig. 6 show a typical example for each of these types): U-shaped warp, i.e. both sides of the disk are warped in the same direction; S-shaped warp with an integral sign-shaped disk plane; $One-side$ warp, i.e. deformations are visible only at one side of the disk; Irr for irregular warp, i.e. completely asymmetric. While the types S and U were described in detail by Reshetnikov & Combes (1998b), it was necessary to introduce One-sided and Irr-shaped warps to enable an adequate description of the observed variety of warped distortions.

The results of this study are summarized in Table 3, distinguishing between the total, non-interacting, and interacting/merging galaxy sample. Accordingly, nearly all ($\approx 93\%$) of the interacting/merging spirals are warped. One third of them shows either U- or S-shaped warps, and nearly another third is warped only at one side. The frequency of warped disks in isolated, non-interacting galaxies is with $\approx 45\%$ unexpectedly high. These galaxies either have S-shaped ($\approx 19\%$) or One-side ($\approx 16\%$) warps, and only 8% of their disks are U-shaped. A correlation between size or type of the warps and morphological type of galaxies was not found.

Finally, it should be stressed that the $\approx 34\%$ of galaxies in the total sample classified as "not warped" are not in contradiction to the previously made conclusion that all galaxy disks investigated are warped (column (4) in Table 2). This is due to the larger tolerances used in the visual inspection of deviations from galactic plane. The results of the classification scheme in Table 3 are therefore qualitative and less sensitive than the measurements listed in column (4) of Table 2.

4. Discussion

The correlation between disk scale height gradients and morphological type of non-interacting galaxies found in this study (gradient -0.006 ± 0.002 in R-band, Sect. 3.1 and Fig. 1) is consistent with results obtained by de Grijs & Pelletier (1997). They found a gradient of -0.0086 ± 0.0012 (I-band) for spiral galaxies with Hubble types between $-2 \leq T \leq 8$. Furthermore, we observe a significant number of galaxies possessing no or very small bulge components but having a large scale height gradient (e.g. NGC 7518). Therefore we can rule out a correlation between the existence of a bulge component and thickened disks. This also supports the results obtained in the two-dimensional study of bulge-disk decomposition by de Grijs & Pelletier (1997). Investigating galaxies with considerable scale height gradients they find that the contribution of the bulge to the total light can be assumed to be negligible (less than 5%). We can also discard an influence of warps on the measured thickness of disks – as proposed by van der Kruit & Searle (1981a) – since this effect was considered in the fitting procedure (Sect. 2).

A more plausible explanation for an increase of disk scale height with radial distance might be either the presence of an underlying thick disk with a scale length comparable or larger than the thin disk (Burstein 1979; de Grijs et al. 1997; de Grijs & Pelletier 1997) or recent accretion of material onto the outer disk parts (Tóth & Ostriker 1992; Quinn et al. 1993; Zaritsky 1995). However, our observations do not sufficiently support the first of these explanations, i.e. the presence of a thick disk. The studied sample only contains a few galaxies with vertical disk profiles weakly indicating the existence of an underlying thick disk. Hence, accretion of small satellites continues to be a promising mechanism in order to explain the origin of gradients in disk scale height.

The size and frequency of tidally-triggered vertical disk perturbations found in this study (Sect. 3 and Table 2) both indicate that such perturbations are typical during a transient phase of close interactions or minor mergers. They likely result from large-scale asymmetries of the gravitational potential, caused by the proximity of the companion (Reshetnikov & Combes 1997). According to results of N-body simulations of minor mergers (Tóth & Ostriker 1992; Walker et al. 1996) the vertical structure of affected disks is mainly characterized by a systematical increase of the scale height towards the outer regions ("slanting" disks) as well as by local instabilities and disk "flaring". Our observations (Figs. 3 and 4) confirm the qualitative predictions of these studies, and the derived statistical results (Table 2) give a quantitative estimate for the size of tidally-triggered perturbations.

The simulations made by Tóth & Ostriker (1992) and Walker et al. (1996) also make some predictions on the lifetime of the evoked perturbations. They conclude that after the encounter the tidally induced perturbations do rapidly decline and the vertically heated disk settles into a new, nearly axisymmetric equilibrium which is stable on longer timescales (> 1 Gyr). This is consistent with the results of this study (columns (2) and (3) in Table 2 and Sect. 3), indicating that tidally-triggered perturbations on large ($\approx R_{\max}$) scales, i.e. gradients in the disk scale height, are common and persistent phenomena if compared to short-lived perturbations on small ($\approx z_0$) scales. Together with the value of ≈ 1.5 found for vertical disk thickening due

to interactions and minor mergers (SDI+II) this is one of the main conclusions of this paper.

Summarizing the results obtained on the size and frequency of stellar warps the high fraction ($\approx 45\%$) of non-interacting galaxies possessing warped distortions is in good agreement with the results of Sanchez-Saavedra et al. (1990) and Reshetnikov & Combes (1998b, Table 1). They found that the fraction of isolated galaxies with warped disks is at least 50% and $(42 \pm 6)\%$, respectively. Assuming a hierarchical galaxy formation scenario it is unrealistic to explain this high fraction of warped disks entirely as a result of tidal interactions in the distant past. Hence we have to consider alternative processes that are able to form new or reinforce existent warps. Possible mechanisms were mentioned in the introduction of this paper. On the other hand, the measured differences in their size – warps of interacting/merging galaxies were found to be at least two times larger than those of non-interacting galaxies on average – indicate that such processes are not capable to produce warps of comparable size. Hence tidal interactions/minor mergers as studied in this paper do at least considerably contribute to the formation and size of warps. According to the results found for our total galaxy sample, the fraction of warped spirals ($\approx 66\%$) is also consistent with a study of stellar warps made by de Grijs (1997), who detected warped disks for $\approx 64\%$ of his objects.

5. Summary and conclusions

A detailed study of the vertical disk structure of 108 highly-inclined/edge-on spiral galaxies was presented. The sample consists of two subsamples of 61 non-interacting and 47 interacting/merging galaxies. In particular, we analyzed the behaviour of the scale height of all disks as a function of galactocentric distance and investigated the properties of vertical, tidally-triggered disk perturbations. Furthermore, the size and frequency of occurrence of warped distortions and bends in galactic disks were studied. The main conlusions are:

1. The scale height of disks of interacting/merging galaxies is characterized by perturbations on both large ($\simeq R_{\rm max}$) and short ($\simeq z_0$) scales. The size of these perturbations are of the order of 280 pc and 130 pc, or 14% and 6% of the corresponding mean scale height, respectively.
2. The scale height of non-interacting galaxies shows similar variations on large (short) scales, with amplitudes of the order of 140 pc (80 pc). This is only about half the size of the perturbations measured for interacting/merging galaxies, and equivalent to 10% and 6% (6% and 4% if corrected for thickened disks) of the corresponding mean scale height, respectively.
3. A hallmark of nearly all disks in the interacting/merging sample is a scale height that increases systematically with radial distance (gradient). The size of these gradients is typically 14% (22% if corrected for thickened disks) of the mean scale height. This is more than twice the value found for non-interacting galaxies.
4. This indicates that tidally-triggered, large-scale disk asymmetries such as scale height gradients are common and persistent phenomena, while local disturbances and bending instabilities decline on shorter timescales.
5. The existence of large scale height gradients for non-interacting, early-type ($T \leq 2$) spirals, weakly dependent on Hubble type, is not associated with the presence of an underlying thick disk. Since many interacting/merging galaxies show the same large gradients, this effect might be due to previous accretion of material or a minor merger.
6. Nearly all (93%) of the interacting/merging and 45% of the non-interacting galaxies investigated are noticeably warped. Down to small amplitudes (≤ 80 pc) all galaxy disks possess warped distortions.
7. Warps of interacting/merging galaxies are $\approx$ 2.5 times larger on average than those observed in non-interacting galaxies, with a mean amplitude of 340 pc and 140 pc, respectively.
8. The results indicate that tidal interactions/minor mergers considerably contribute to the formation and size of warps. However, these processess cannot entirely explain the observed frequent occurrence of warped disks.

Acknowledgements. The authors would like to thank the referee of this paper, Dr. J.A. Sellwood, for his useful comments and suggestions, and M. R. Corbin for his careful reading of the manuscript.
This work was supported by a *Lynen* fellowship of the *Alexander von Humboldt Foundation* and by the *Deutsche Forschungsgemeinschaft* (DFG) under grants no. De 385 and GRK 118.
This research has made use of the NASA/IPAC Extragalactic Database (NED) which is operated by the Jet Propulsion Laboratory, California Institute of Technology, under contract with the National Aeronautics and Space Administration.

References

Barnaby D., Thronson H.A. Jr., 1992, AJ 103, 41
Battaner E., Florido E., Sanchez-Saavedra M.L., 1990, A&A 236, 1
Binney J., 1981, MNRAS 196, 455
Binney J., 1992, ARAA 30, 51
Burstein D., 1979, ApJ 234, 829
Barteldrees A., Dettmar R.-J., 1994, A&AS 103, 475
Fall S.M, Efstathiou G., 1980, MNRAS 193, 189
Grijs R. de, 1997, PhD Thesis, Rijksuniversiteit Groningen
Grijs R. de, Kruit P.C. van der, 1996, A&AS 117, 19
Grijs R. de, Pelletier R.F., 1997, A&A 320, L21
Grijs R. de, Pelletier R.F., Kruit P.C. van der, 1997, A&A 327, 986
Griv E., Peter W., 1996, ApJ 469, 84

Griv E., Peter W., 1996, ApJ 469, 99
Griv E., Peter W., 1996, ApJ 469, 103
Kruit P.C. van der, Searle L., 1981a, A&A 95, 105
Kruit P.C. van der, Searle L., 1981b, A&A 95, 116
Kruit P.C. van der, Searle L., 1982a, A&A 110, 61
Mihos J.C., Walker I.R., Herquist L., 1995, ApJ 447, L87
Pfenniger D., Combes F., Martinet L., 1994, A&A 285, 79
Quinn P.J., Hernquist L., Fullagar D.P., 1993, ApJ 403, 74
Reshetnikov V., Combes F., 1996, A&AS 116, 417
Reshetnikov V., Combes F., 1997, A&A 324, 80
Reshetnikov V., Combes F., 1998, A&A 337, 9
Reshetnikov V., Combes F., 1998, A&AS 138, 110
Sanchez-Saavedra M. L., Battaner E., Florido, E., 1990, MNRAS 246, 458
Schwarz U.J., 1985, A&A 142, 273
Schwarzkopf U., 1999, Ph.D. Thesis, Ruhr-University Bochum
Schwarzkopf U., Dettmar R.-J., 2000a, A&AS 144, 85, Paper I
Schwarzkopf U., Dettmar R.-J., 2000b, A&A 361, 451, Paper II
Sellwood J.A., 1996, ApJ 473, 733
Shaw M.A., Gilmore G., 1990, MNRAS 242, 59
Sparke L., 1984, NNRAS 211, 911
Sparke L., Casertano S., 1988, MNRAS 234, 873
Spitzer L., Schwarzschild M., 1951, ApJ 114, 385
Tóth G., Ostriker J.P., 1992, ApJ 389, 5
Verdes-Montenegro L., Yun M.S., Ho P.T.P, 1998, ApJ 497, 89
Wainscoat R.J., Freeman K.C., Hyland A.R., 1989, ApJ 337, 163
Walker I.R., Mihos C., Hernquist L., 1996, ApJ 460, 121
Zaritsky D., 1995, ApJ 448, L17
Zaritsky D., Rix, H.-W., 1997, ApJ 477, 118
Zepf S.E., 1993, ApJ 407, 448

Table 4. Parameters obtained by an analysis of the vertical disk structure (based on R-band data of SDI+II, Tables 4 and 5). Columns: (1) Serial number; (2) Galaxy name; (3) Best-fitting / Alternative vertical disk model: $1 = \exp, 2 = \mathrm{sech}, 3 = \mathrm{sech}^2$; (4) Mean value of disk scale height z_0; (5) Gradient of the first-order scale height fit (average from both disk sides), and its error; (6) – (8): Standard deviation (in pc and in percent of its mean value $(z_0)_{\mathrm{mean}}$) of: (6) ... mean disk scale height; (7) ... first-order scale height fit; (8) ... average galactic plane, i.e. disk warping; (9) Goodness-of-fit parameter, defined as the difference between observations and fit (for a detailed explanation of fit parameters see Sect. 2).

No.	Galaxy	Vertical Fit		$(z_0)_{\mathrm{mean}}$		$(z_0)_{\mathrm{grad}}$		$(z_0)_{\mathrm{std}}$		$(z_0)_{\mathrm{std1}}$		Warping		Q
		Best	Alt.	[″]	[kpc]	$[10^{-3}]$		[pc]	[%]	[pc]	[%]	[pc]	[%]	
(1)	(2)	(3)		(4)		(5)		(6)		(7)		(8)		(9)
Interacting / Merging														
1	NGC 7	3	2	8.4	0.81	55	± 5	76	9.5	35	4.3	117	14.4	1.23
2	UGC 260	2	–	10.0	1.54	−9	± 2	70	4.5	60	3.9	145	9.4	3.32
3	NGC 128	2	1	11.5	3.34	15	± 4	690	20.7	62	1.9	568	17.0	2.92
4	AM 0107-375	2	–	3.1	—	75	± 11	—	22.1	—	6.4	—	13.2	1.14
5	ESO 296-G17	2	–	6.9	2.80	55	± 5	242	8.6	116	4.1	209	7.5	3.26
6	ESO 354-G05	2	–	3.1	—	38	± 7	—	10.4	—	5.7	—	10.4	1.46
7	ESO 245-G10	2	–	8.3	3.20	46	± 4	267	8.3	89	2.8	317	9.9	6.45
8	ESO 417-G08	2	–	8.5	2.80	−27	± 4	302	10.8	218	7.8	377	13.5	1.79
9	ESO 199-G12	2	–	4.0	1.87	20	± 6	230	12.3	117	6.3	373	19.9	2.76
10	ESO 357-G16	2	–	5.7	0.50	28	± 5	40	8.0	23	4.6	50	9.9	1.71
11	ESO 357-G26	1	–	19.0	1.69	103	± 6	229	13.6	61	3.6	160	9.5	4.89
12	ESO 418-G15	2	–	10.2	0.68	10	± 3	36	5.3	12	1.8	131	19.3	3.85
13	NGC 1531/32	1	2	64.4	4.99	93	± 14	930	18.6	674	13.5	791	15.9	6.91
14	ESO 202-G04	2	–	8.0	0.57	114	± 5	66	11.6	21	3.7	51	9.0	1.92
15	ESO 362-G11	1	–	10.7	0.99	49	± 14	156	15.8	74	7.5	115	11.6	1.61
16	NGC 1888	2	–	13.6	2.10	88	± 8	453	21.6	148	7.0	585	27.8	9.60
17	ESO 363-G07	1	–	12.1	1.10	52	± 3	128	11.6	37	3.4	65	5.9	2.31
18	ESO 487-G35	3	2	8.6	0.98	38	± 10	152	15.5	92	9.4	182	18.6	4.68
19	NGC 2188	1	–	21.1	1.18	52	± 10	131	11.1	82	6.9	244	20.7	5.89
20	UGC 3697	2	–	3.3	0.69	4	± 3	77	11.2	22	3.2	215	31.1	1.81
21	ESO 060-G24	2	–	9.0	2.51	113	± 15	500	19.9	236	9.4	8	0.3	2.52
22	ESO 497-G14	2	–	6.8	1.50	54	± 11	166	11.1	89	5.9	134	8.9	2.54
23	NGC 3044	1	–	11.3	1.17	13	± 14	183	15.6	110	9.4	243	20.7	4.83
24	NGC 3187	3	1	23.5	2.85	227	± 11	727	25.5	223	7.8	561	19.7	3.30
25	ESO 317-G29	1	2	18.9	3.16	−3	± 34	232	7.3	121	3.8	83	2.6	2.73
26	ESO 264-G29	2	–	6.0	1.33	44	± 2	493	37.1	129	9.7	780	58.7	5.29
27	NGC 3432	1	–	17.6	0.90	23	± 7	125	13.9	43	4.8	324	36.0	2.67
28	NGC 3628	2	–	55.8	1.30	59	± 5	105	8.1	47	3.6	157	12.1	8.00
29	ESO 378-G13	2	–	4.7	—	72	± 16	—	13.2	—	7.9	—	19.3	0.82
30	ESO 379-G20	3	2	3.0	2.82	33	± 9	726	25.7	197	7.0	1479	52.5	6.30
31	NGC 4183	2	–	8.1	0.69	70	± 20	66	9.6	46	6.7	74	10.8	6.47
32	NGC 4631	1	–	34.1	1.32	31	± 22	299	22.7	130	9.8	178	13.5	6.95
33	NGC 4634	1	–	11.4	0.88	116	± 5	190	21.6	55	6.3	98	11.2	1.18
34	NGC 4747	1	–	16.1	1.75	101	± 4	232	13.3	62	3.5	254	14.5	1.59
35	NGC 4762	3	2	28.1	1.59	46	± 38	364	22.9	299	18.8	311	19.5	4.10
36	ESO 443-G21	2	–	5.1	0.95	2	± 4	103	10.8	101	10.6	83	8.8	2.43
37	NGC 5126	2	–	6.7	2.09	−9	± 7	183	8.8	155	7.4	125	6.0	0.90
38	ESO 324-G23	2	1	14.3	1.85	91	± 8	372	20.1	97	5.2	550	29.7	6.49
39	ESO 383-G05	1	–	15.4	3.73	−45	± 2	518	13.9	191	5.1	383	10.3	2.40
40	NGC 5297	3	2	9.0	1.65	34	± 8	103	6.2	67	4.1	212	12.9	2.13
41	ESO 445-G63	2	–	7.6	—	84	± 25	—	26.6	—	9.7	—	7.6	2.02
42	NGC 5529	1	–	8.0	1.43	51	± 3	227	15.9	81	5.7	254	17.7	3.32
43	NGC 5965	1	–	9.1	2.02	−1	± 6	203	10.0	132	6.5	296	14.6	1.12
44	NGC 6045	2	1	4.5	2.88	89	± 13	476	16.5	271	9.4	1388	48.2	0.80
45	NGC 6361	3	1	9.7	2.49	−9	± 2	117	4.7	101	4.1	242	9.7	2.51
46	Arp 121	2	–	7.9	2.89	123	± 14	466	16.1	197	6.8	804	27.8	3.99
47	IC 4991	3	–	2.5	0.95	0	± 8	103	10.8	73	7.7	182	19.2	4.43

Table 4. (continued)

No.	Galaxy	Vertical Fit		$(z_0)_{\rm mean}$		$(z_0)_{\rm grad}$	$(z_0)_{\rm std}$		$(z_0)_{\rm std1}$		Warping		Q
		Best	Alt.	[″]	[kpc]	[10^{-3}]	[pc]	[%]	[pc]	[%]	[pc]	[%]	
(1)	(2)	(3)		(4)		(5)	(6)		(7)		(8)		(9)
Non − Interacting													
1	UGC 231	2	3	8.6	0.57	10 ± 5	41	7.2	36	6.3	31	5.5	1.57
2	ESO 150-G07	1	2	5.4	—	41 ± 13	—	9.5	—	3.5	—	6.4	1.26
3	ESO 112-G04[a)]	2	–	2.1	—	−5 ± 7	—	24.2	—	18.8	—	17.3	0.99
4	ESO 150-G14[a)]	2	–	4.9	2.73	19 ± 8	300	11.0	235	8.6	357	13.1	1.04
5	UGC 711	2	–	7.0	0.92	22 ± 7	116	12.6	46	5.0	67	7.3	1.20
6	ESO 244-G48	1	–	6.3	—	3 ± 3	—	1.7	—	1.3	—	3.7	0.75
7	UGC 1839	2	–	8.0	0.80	2 ± 15	110	13.8	95	11.9	117	14.6	3.00
8	NGC 891	2	–	23.8	1.10	−8 ± 9	79	7.2	56	5.1	84	7.6	2.61
9	ESO 416-G25[a)]	3	2	4.7	1.56	21 ± 7	296	19.0	135	8.7	93	6.0	4.71
10	UGC 2411	2	–	6.2	1.13	5 ± 20	455	40.3	343	30.4	217	19.2	1.91
11	IC 1877	2	3	2.1	—	−9 ± 5	—	11.6	—	8.0	—	10.7	4.63
12	ESO 201-G22	2	–	4.2	1.17	−1 ± 3	105	9.0	53	4.5	120	10.3	4.16
13	NGC 1886	2	–	5.8	0.67	9 ± 4	73	10.9	18	2.7	58	8.6	2.99
14	UGC 3474	2	–	4.2	1.03	−35 ± 7	124	12.0	50	4.9	70	6.8	0.74
15	NGC 2310	3	2	9.3	0.83	26 ± 4	77	9.3	34	4.1	158	19.0	3.39
16	UGC 4278	2	–	5.8	0.31	4 ± 2	13	4.2	7	2.3	102	32.9	3.87
17	ESO 564-G27[a)]	3	2	5.2	0.83	−2 ± 6	189	22.8	118	14.2	59	7.1	1.92
18	UGC 4943	2	–	2.1	0.34	12 ± 5	36	10.6	20	5.9	47	13.8	1.21
19	IC 2469	1	–	16.2	1.75	9 ± 6	132	7.5	118	6.7	397	22.2	3.40
20	UGC 5341	2	–	4.0	1.87	0 ± 4	188	10.1	115	6.1	257	13.7	1.39
21	IC 2531	3	2	10.4	1.67	52 ± 24	544	32.6	469	28.1	381	22.8	8.61
22	NGC 3390	1	–	11.0	2.02	29 ± 9	285	14.1	78	3.9	162	8.0	5.65
23	ESO 319-G26[a)]	3	–	2.4	0.48	5 ± 11	79	16.5	60	12.5	135	28.2	2.09
24	NGC 3957	1	–	9.3	1.33	30 ± 8	132	9.9	94	7.1	108	8.1	4.28
25	NGC 4013	1	–	11.7	0.68	2 ± 7	35	5.1	31	4.6	34	5.0	1.65
26	ESO 572-G44	1	–	7.0	3.03	47 ± 3	221	7.3	85	2.8	159	5.3	0.41
27	UGC 7170	2	–	3.0	0.43	0 ± 3	20	4.7	18	4.2	42	9.8	1.61
28	ESO 321-G10[a)]	1	–	4.9	1.00	6 ± 3	49	4.9	43	4.3	60	6.0	1.36
29	NGC 4217	2	–	21.7	1.53	35 ± 5	148	9.7	56	3.7	145	9.5	3.63
30	NGC 4244	2	–	22.1	0.41	48 ± 22	71	17.3	50	12.2	67	16.4	8.16
31	UGC 7321	2	–	4.9	0.38	−2 ± 4	28	7.4	24	6.3	44	11.7	2.72
32	NGC 4302	2	–	8.1	0.62	39 ± 3	52	8.4	22	3.5	72	11.6	0.81
33	NGC 4330	1	–	16.6	1.27	75 ± 9	176	13.9	86	6.8	110	8.6	1.71
34	NGC 4565	1	–	10.7	0.52	−7 ± 2	36	6.9	24	4.6	53	10.2	2.04
35	NGC 4710	1	2	11.6	0.81	60 ± 9	76	9.4	42	5.2	60	7.4	1.38
36	NGC 5170	1	–	22.1	1.69	−37 ± 26	219	13.0	121	7.2	247	14.6	2.39
37	ESO 510-G18	2	–	1.0	—	14 ± 1	—	11.3	—	1.2	—	10.4	0.54
38	UGC 9242	1	–	5.7	0.70	−12 ± 11	173	24.7	65	9.3	40	5.7	1.81
39	NGC 5775	1	–	13.5	1.90	29 ± 10	218	11.5	142	7.5	87	4.6	2.95
40	NGC 5907	2	–	18.2	0.97	7 ± 7	106	10.9	60	6.2	94	9.7	4.74
41	NGC 5908	2	–	8.9	1.92	−19 ± 9	192	10.0	156	8.1	126	6.6	1.39
42	ESO 583-G08	2	–	1.7	0.84	10 ± 2	66	7.9	34	4.0	117	14.0	0.53
43	NGC 6181	2	–	5.2	0.91	59 ± 6	88	9.7	36	4.0	70	7.7	1.53
44	ESO 230-G11	3	–	3.8	1.28	−6 ± 5	96	7.5	90	7.0	348	27.2	1.53
45	NGC 6722[a)]	1	–	7.9	2.53	−16 ± 9	186	7.4	78	3.1	291	11.5	2.03
46	ESO 461-G06	1	–	3.0	—	−27 ± 13	—	11.8	—	5.4	—	4.8	1.43
47	ESO 339-G16[a)]	2	–	4.5	—	81 ± 2	—	18.2	—	3.3	—	6.9	0.29
48	IC 4937[a)]	3	2	5.4	1.66	−3 ± 2	101	6.1	79	4.8	200	12.1	1.04
49	ESO 187-G08	2	3	3.3	1.02	8 ± 3	139	13.6	105	10.3	182	17.8	0.68
50	IC 5052	1	–	19.3	0.75	38 ± 10	117	15.6	86	11.5	101	13.5	1.96
51	IC 5096[b)]	1	–	6.5	1.46	—	—	—	—	—	—	—	—

Table 4. (continued)

No.	Galaxy	Vertical Fit		$(z_0)_{\rm mean}$		$(z_0)_{\rm grad}$	$(z_0)_{\rm std}$		$(z_0)_{\rm std1}$		Warping		Q
		Best	Alt.	[″]	[kpc]	[10^{-3}]	[pc]	[%]	[pc]	[%]	[pc]	[%]	
(1)	(2)	(3)		(4)		(5)	(6)		(7)		(8)		(9)
52	ESO 466-G01[a)]	1	–	6.8	3.24	4 ± 4	319	9.8	95	2.9	333	10.3	0.42
53	ESO 189-G12	1	–	3.60	2.03	19 ± 12	270	11.7	191	8.3	330	16.2	1.82
54	UGC 11859[a)]	1	–	1.5	0.32	-15 ± 2	50	15.6	29	9.1	57	17.8	0.45
55	ESO 533-G04	1	–	7.6	1.40	41 ± 6	158	11.3	86	6.1	146	10.5	1.25
56	IC 5199	1	–	5.0	1.72	20 ± 5	70	4.1	62	3.6	145	8.4	2.44
57	UGC 11994	2	3	4.0	1.37	18 ± 2	116	8.5	79	5.8	208	15.2	1.23
58	UGC 12281	2	–	5.7	1.09	-15 ± 6	107	9.8	54	5.0	174	16.0	3.83
59	UGC 12423	1	–	7.9	2.69	28 ± 16	796	29.6	277	10.3	229	8.5	1.22
60	NGC 7518	1	–	9.6	2.44	149 ± 8	472	19.3	171	7.0	296	12.1	3.02
61	ESO 604-G06	2	–	3.4	1.74	3 ± 2	150	8.6	138	7.9	147	8.5	1.08

[a)] Supplementary data from Barteldrees & Dettmar (1994).
[b)] No fit was performed. Disk parameters were taken from Table 5 in SD II.

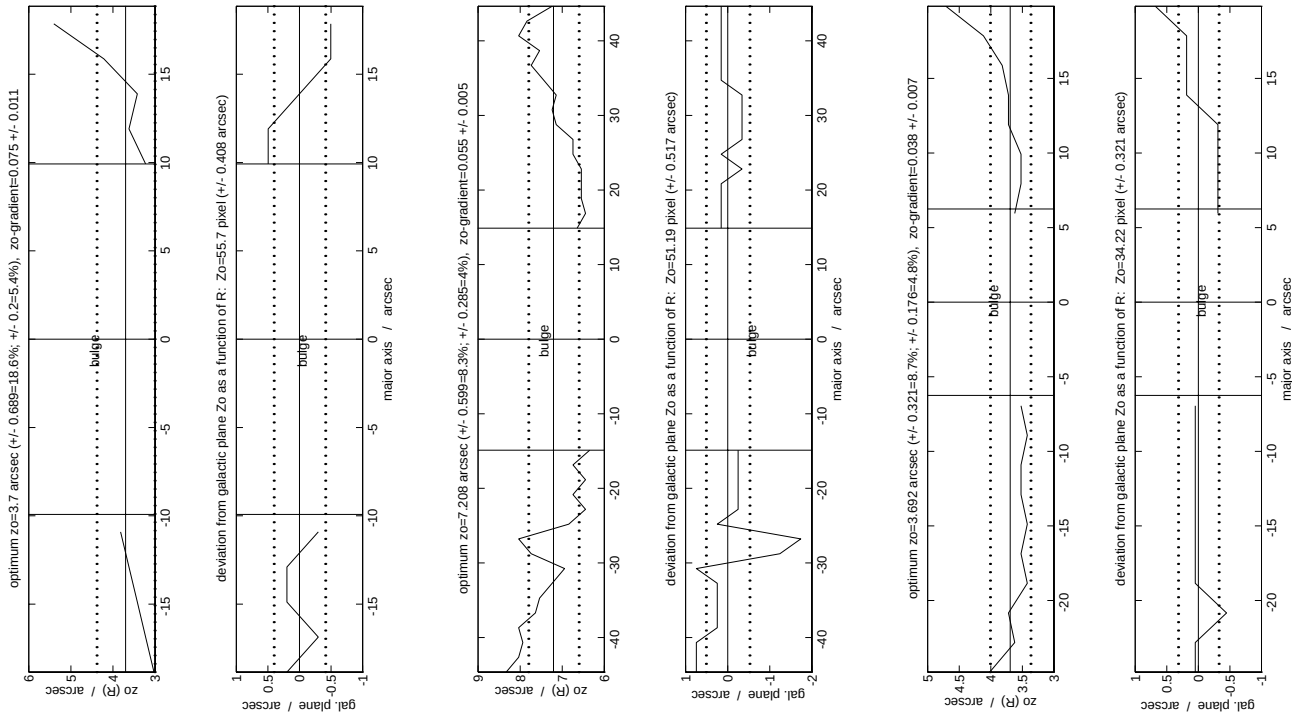

AM0107-375 ESO 296-G17 ESO 354-G05

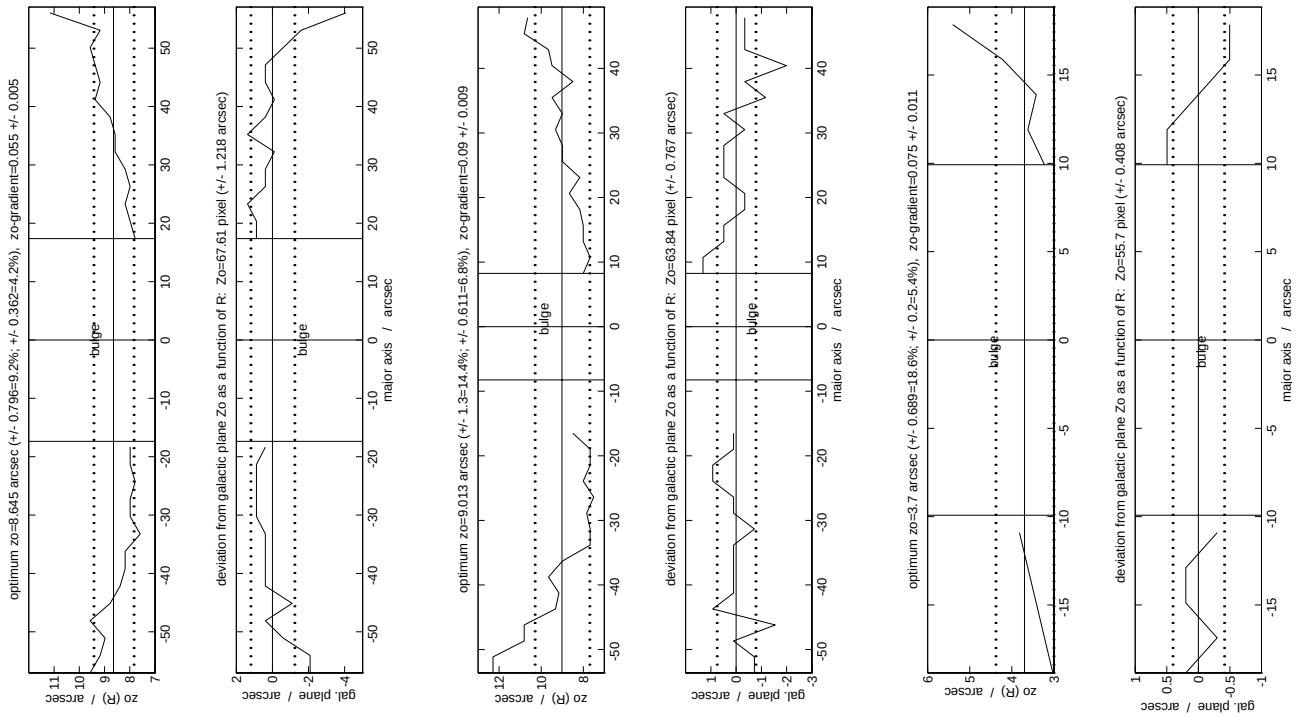

NGC 7 UGC 260 NGC 128

Appendix A. The measured behaviour of scale height (upper panels) and mean galactic plane (lower panels) along the major axis of the disk, shown for each galaxy in the interacting/merging sample. The main output parameters are indicated. For details see Sect. 3 and Table 4 in this paper. Contour maps were given in Paper I, Figs. 4 and 5.

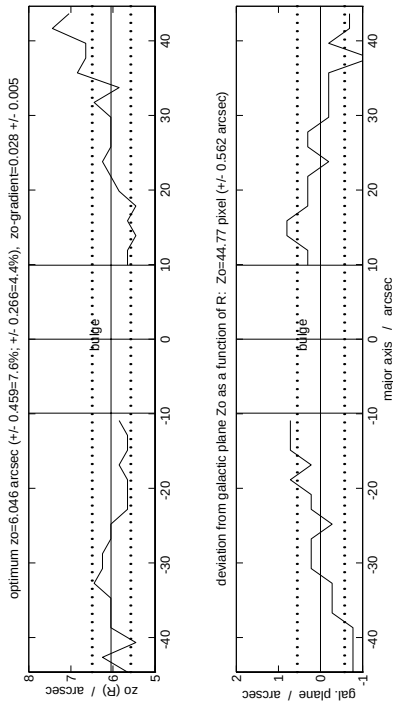

ESO 357-G16

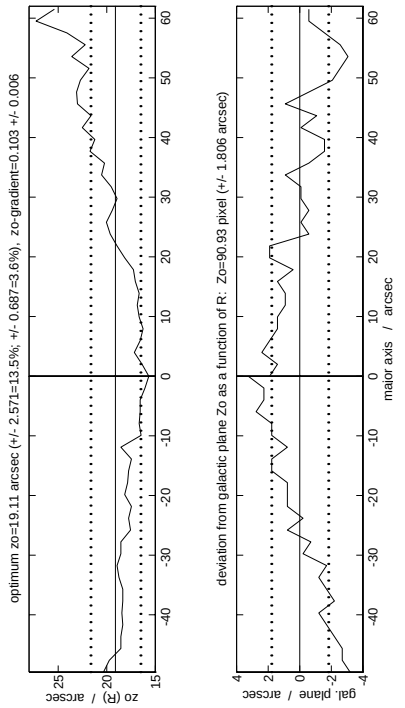

ESO 357-G26

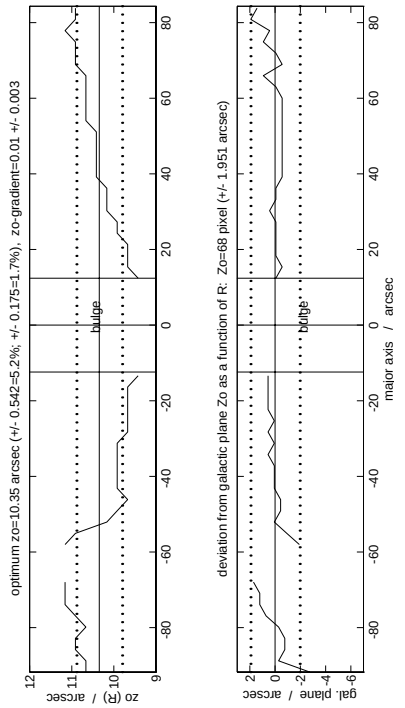

ESO 418-G15

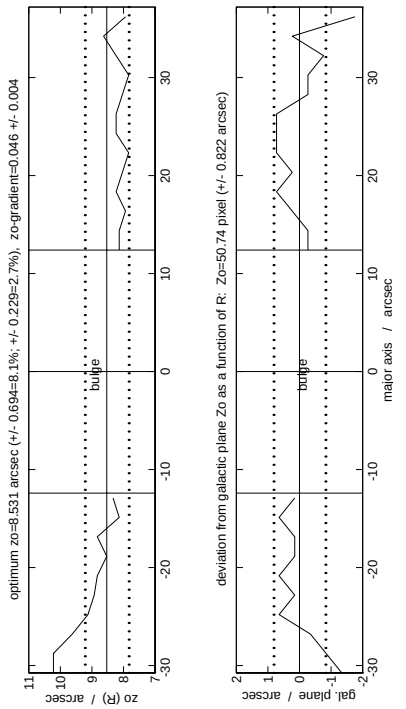

ESO 245-G10

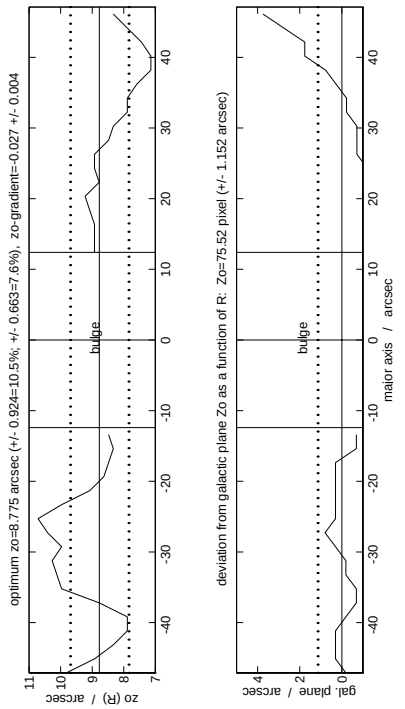

ESO 417-G08

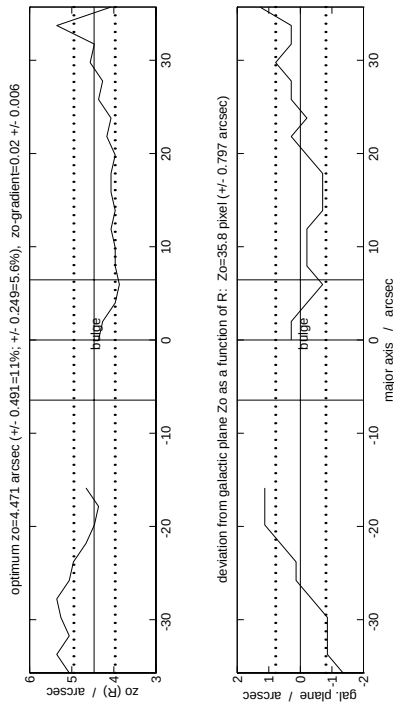

ESO 199-G12

Appendix A. (continued)

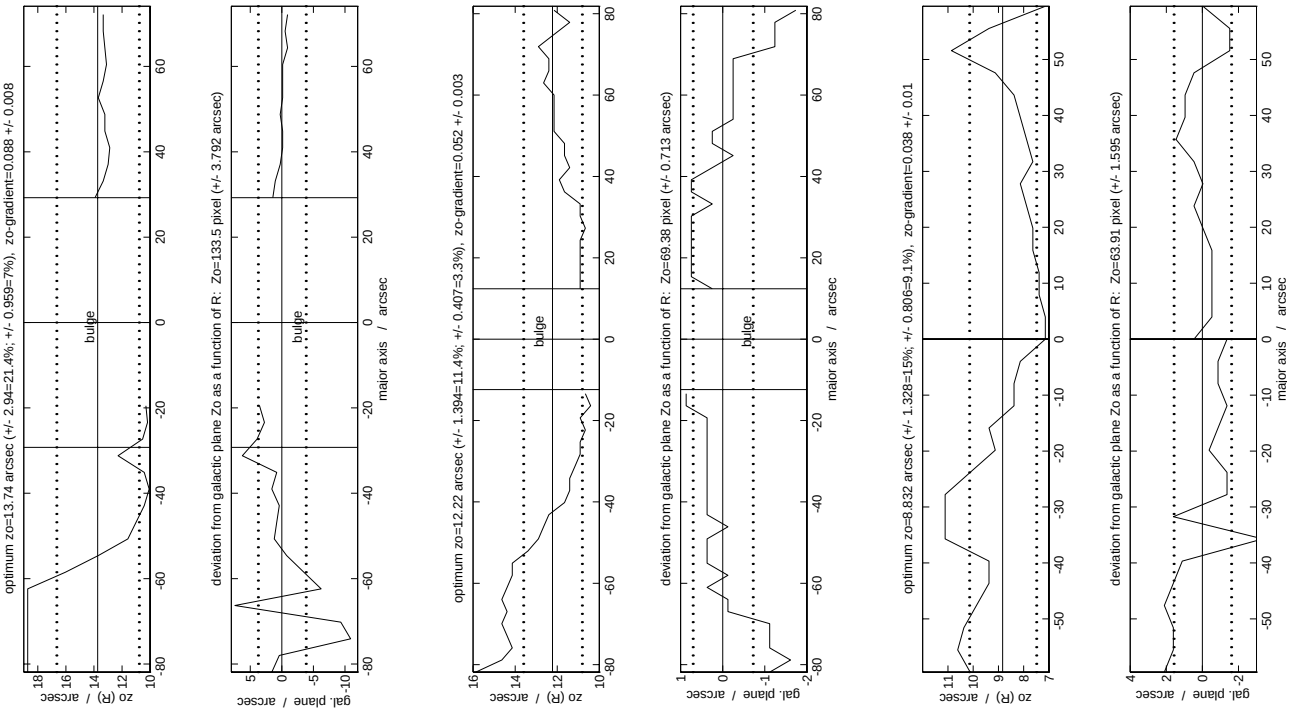

NGC 1888 ESO 363-G07 ESO 487-G35

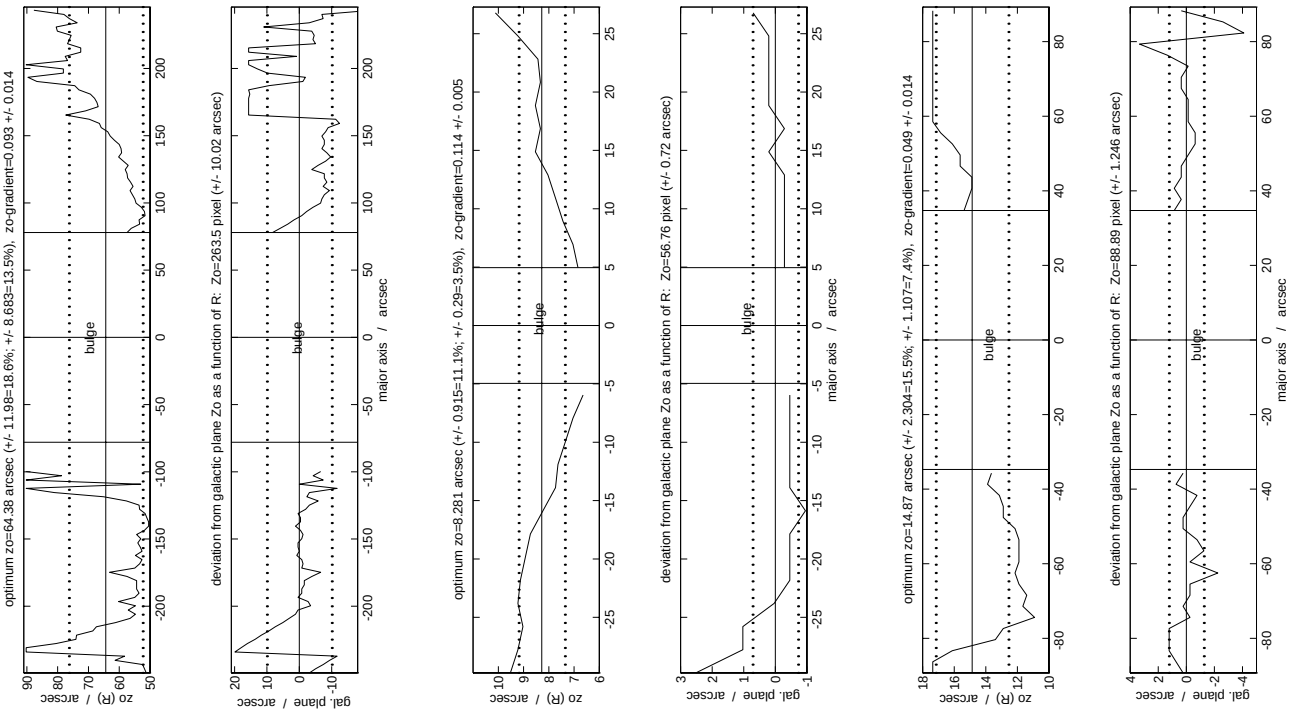

NGC 1531 ESO 202-G04 ESO 362-G11

Appendix A. (continued)

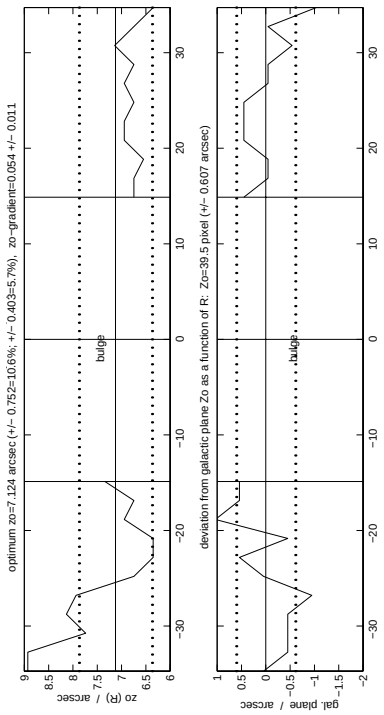

ESO 497-G14

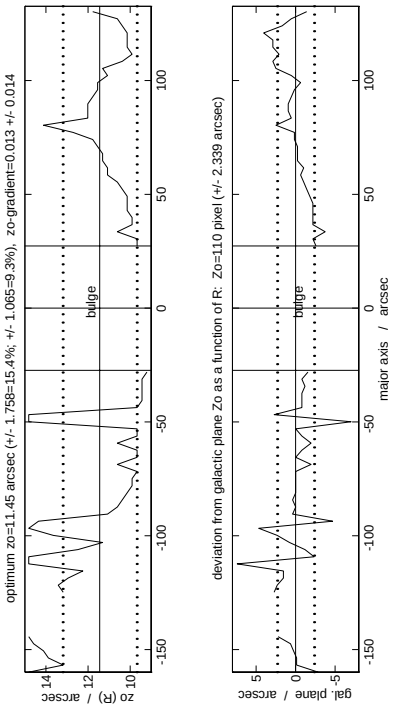

NGC 3044

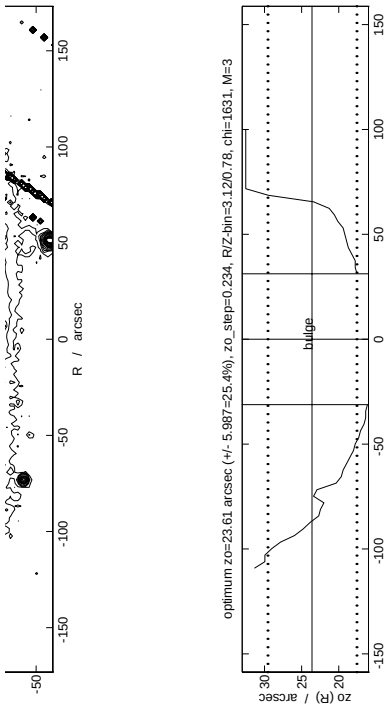

NGC 3187

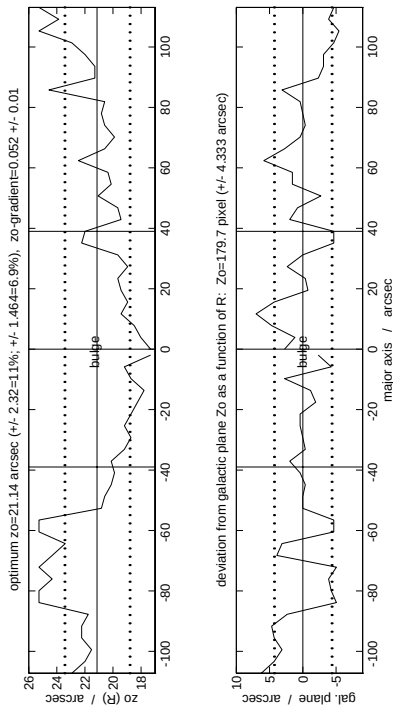

NGC 2188

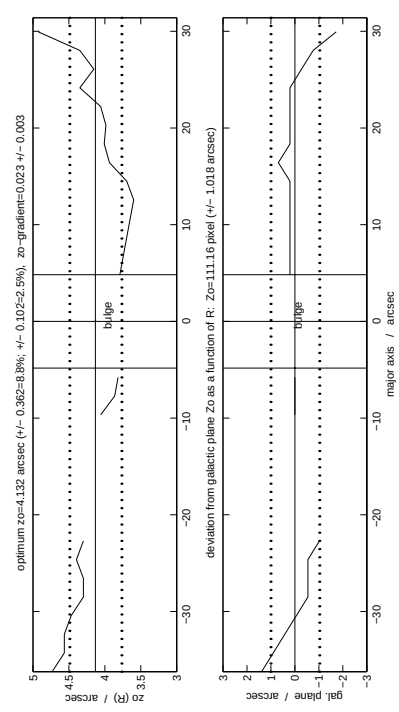

UGC 3697

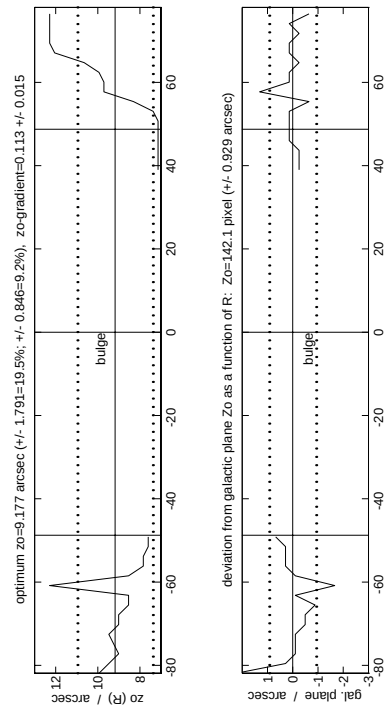

ESO 060-G24

Appendix A. (continued)

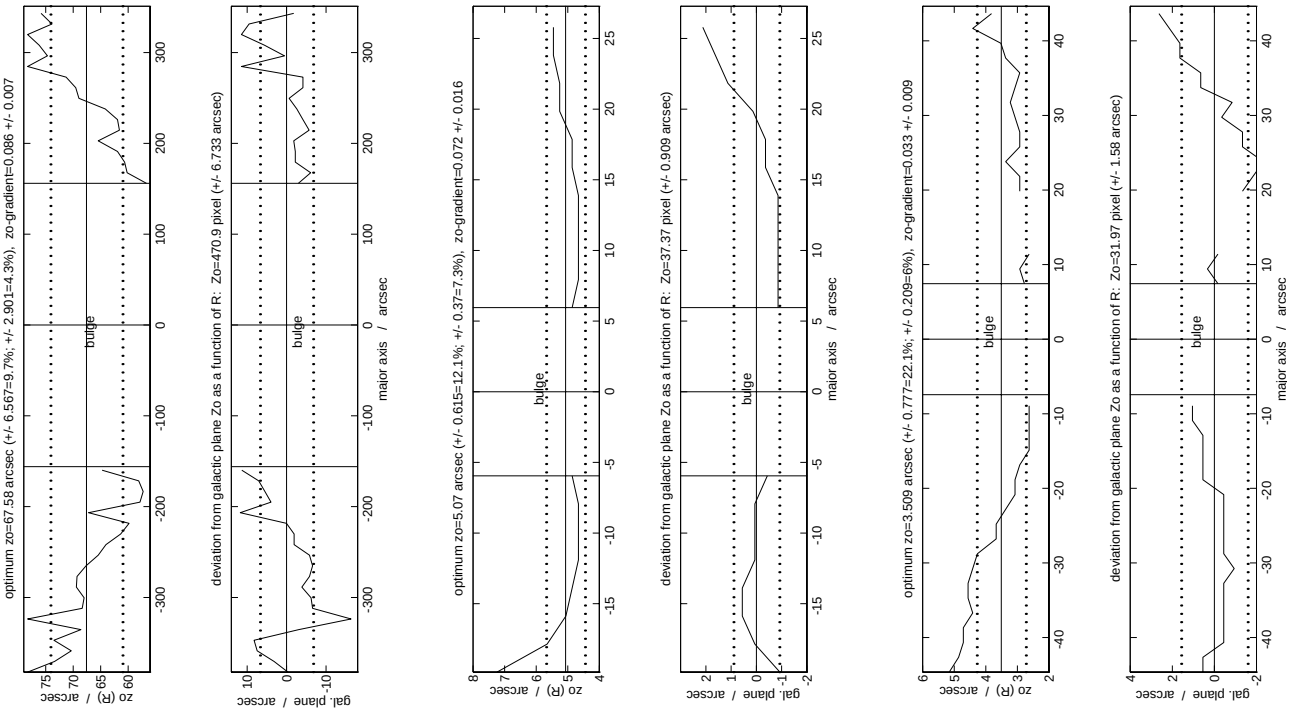

NGC 3628 ESO 378-G13 ESO 379-G20

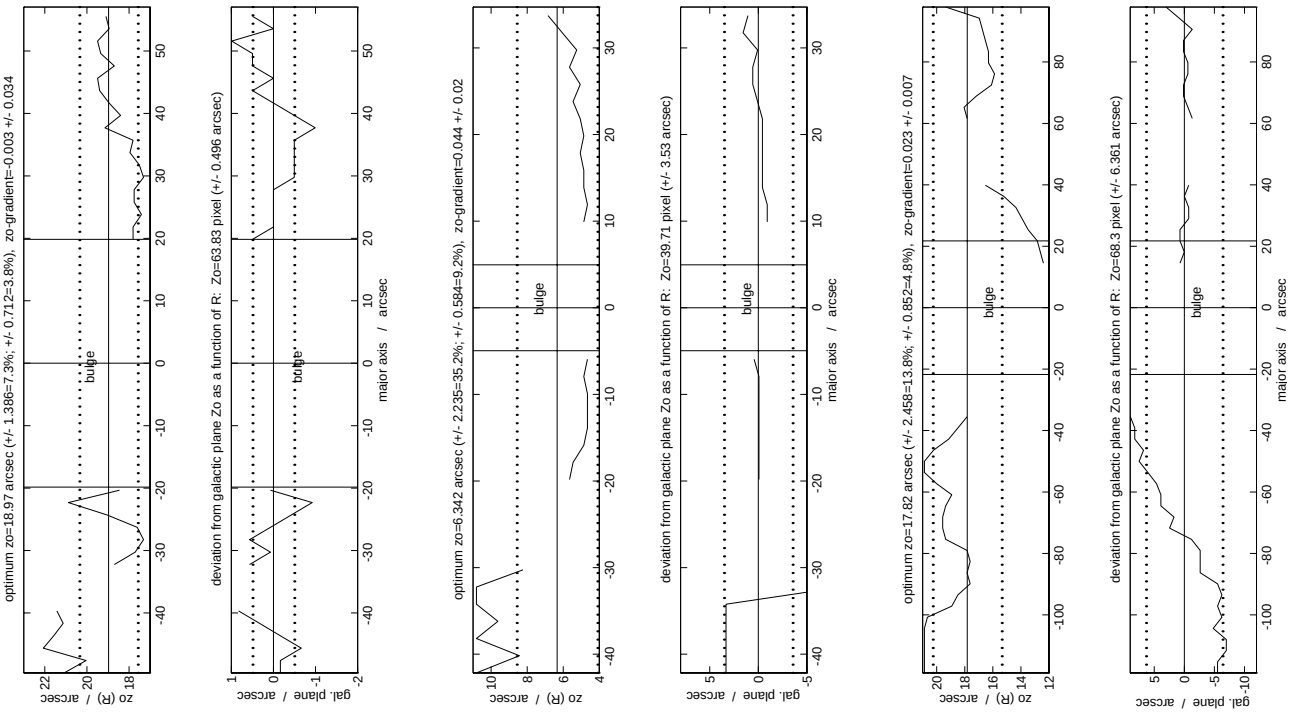

ESO 317-G29 ESO 264-G29 NGC 3432

Appendix A. (continued)

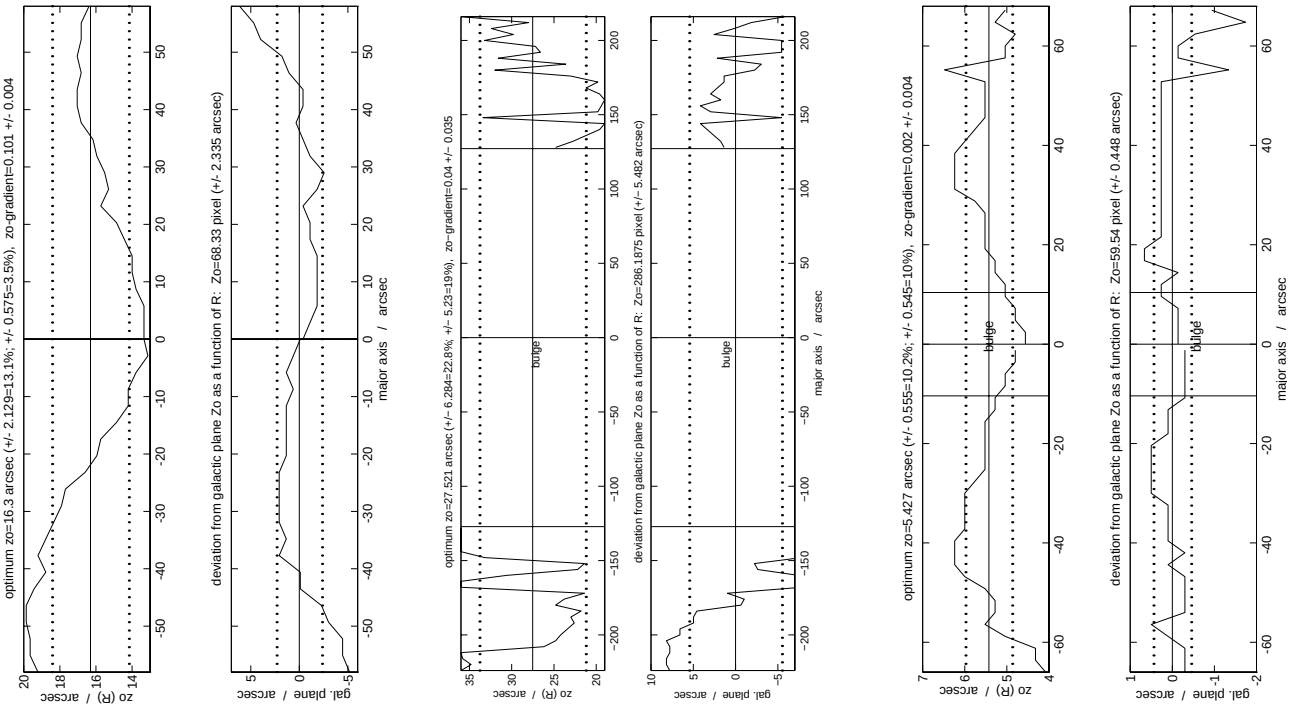

NGC 4747 NGC 4762 ESO 443-G21

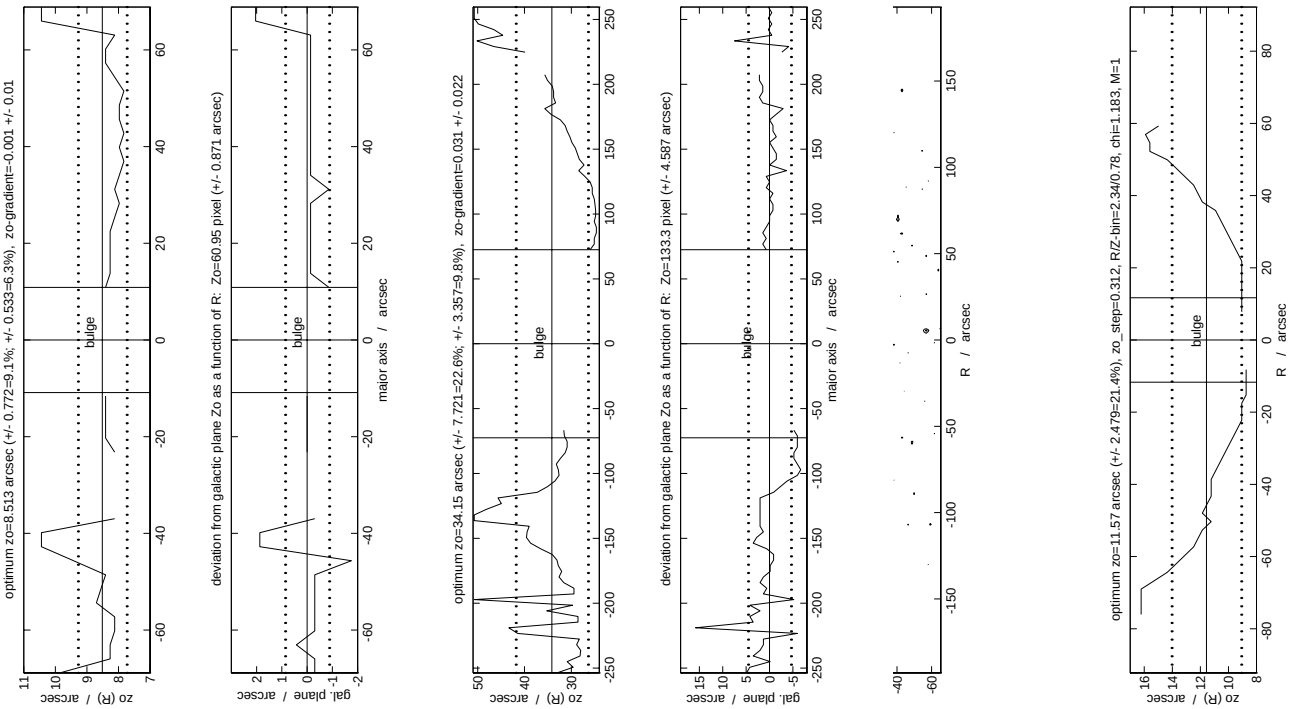

NGC 4183 NGC 4631 NGC 4634

Appendix A. (continued)

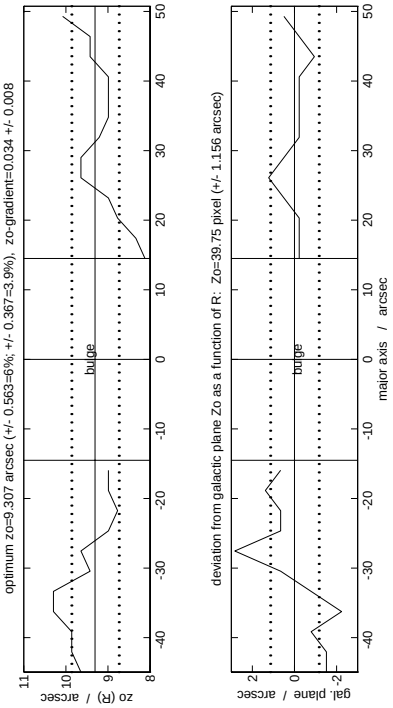

NGC 5297

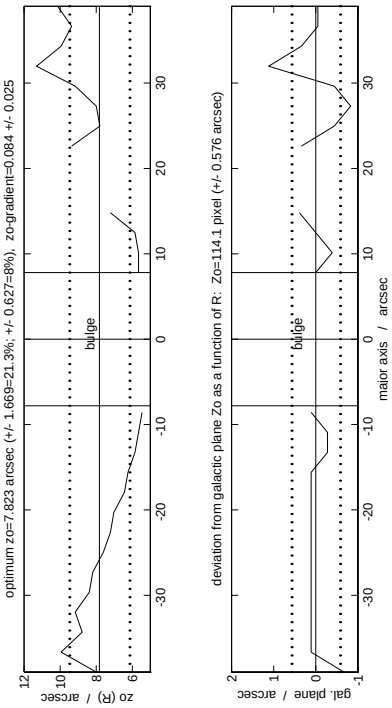

ESO 445-G63

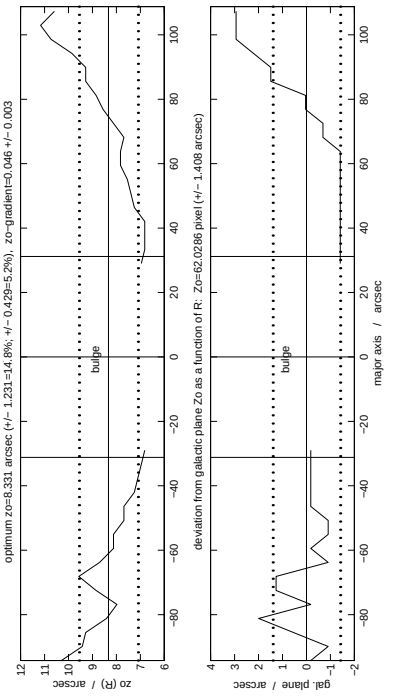

NGC 5529

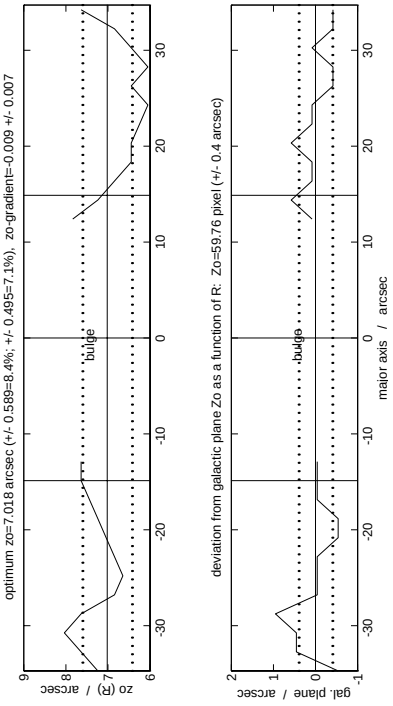

NGC 5126

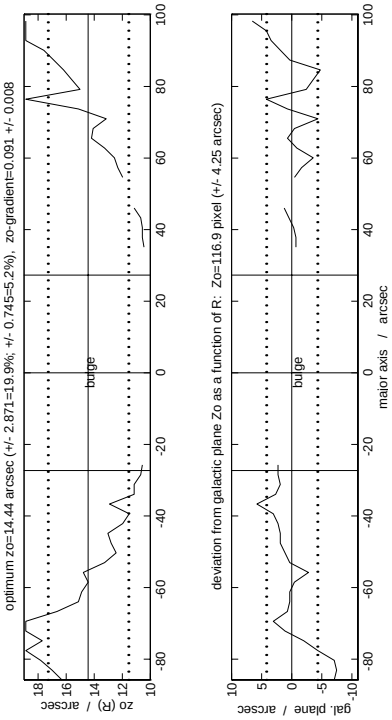

ESO 324-G23

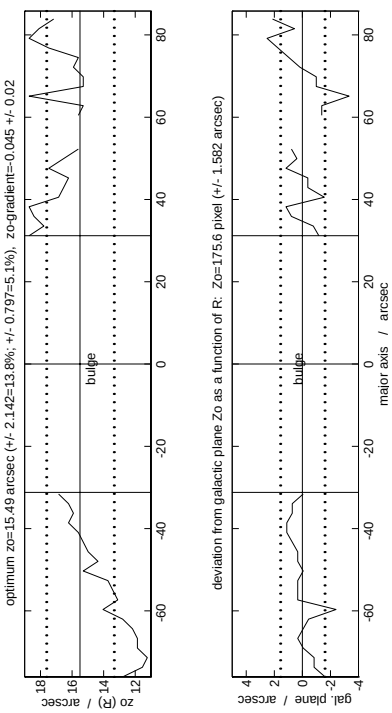

ESO 383-G05

Appendix A. (continued)

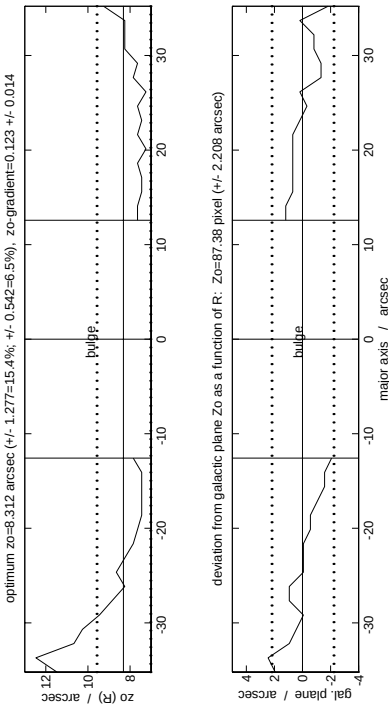

Arp 121

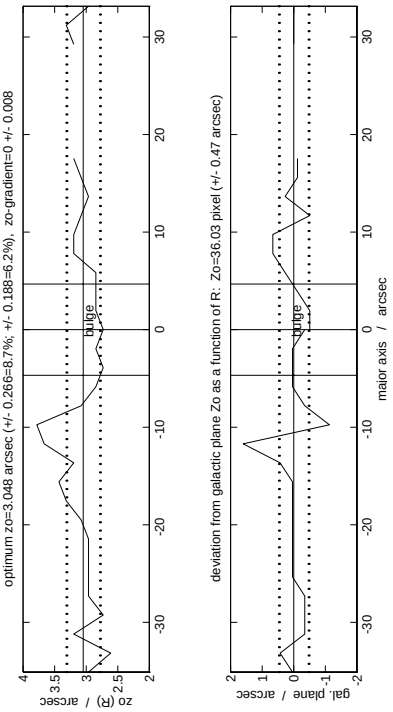

IC 4991

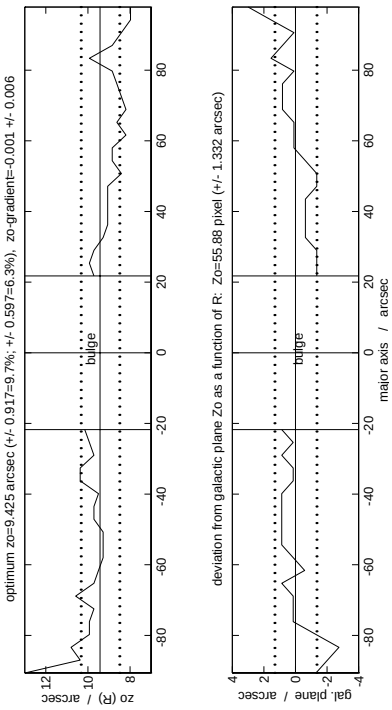

NGC 5965

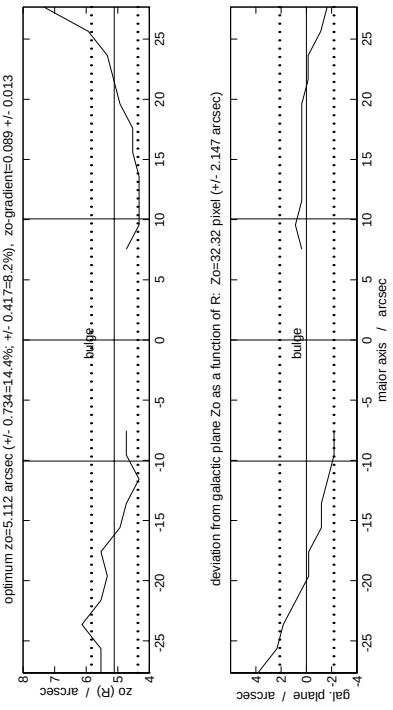

NGC 6045

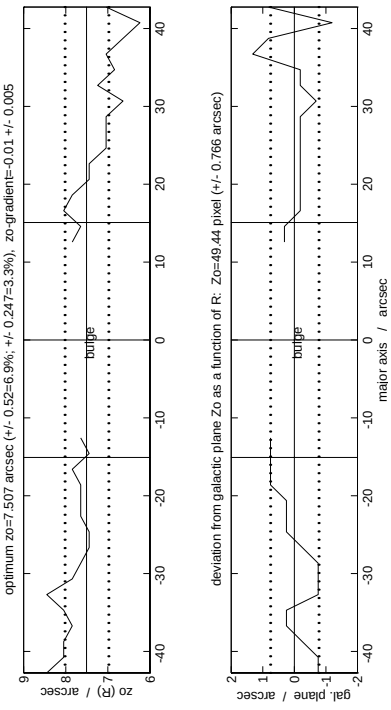

NGC 6361

Appendix A. (continued)

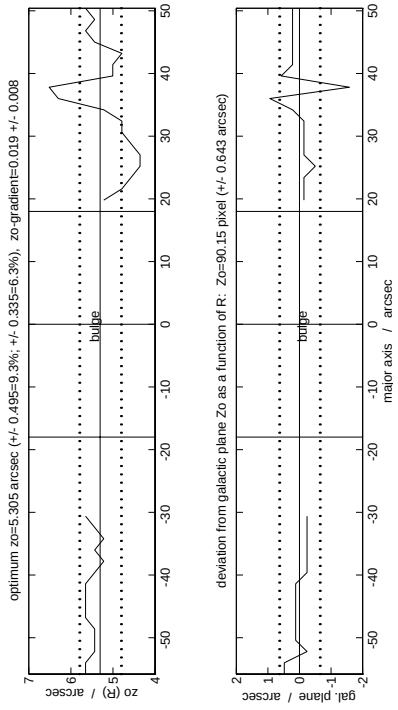

ESO 150-G14

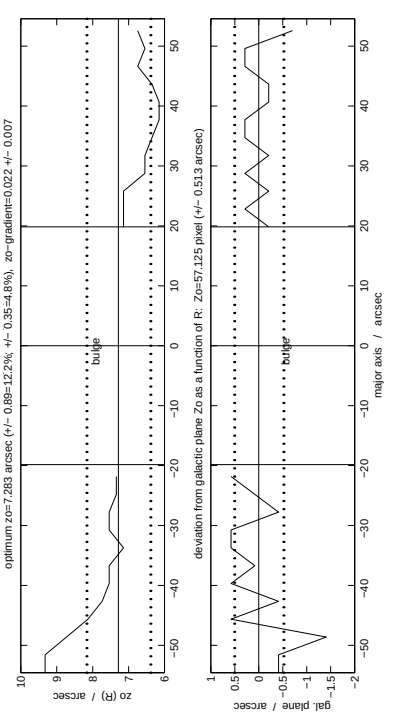

UGC 711

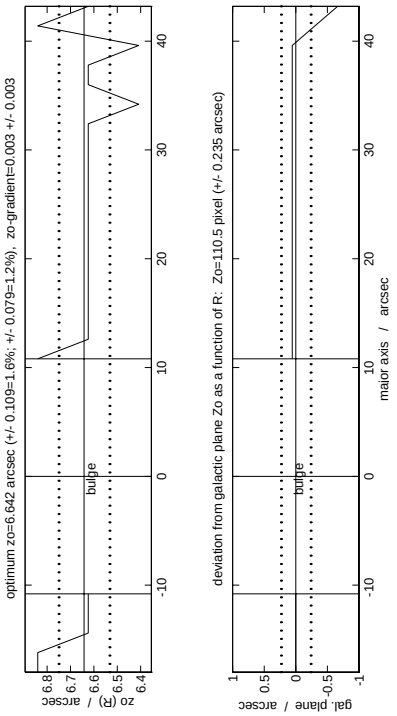

ESO 244-G48

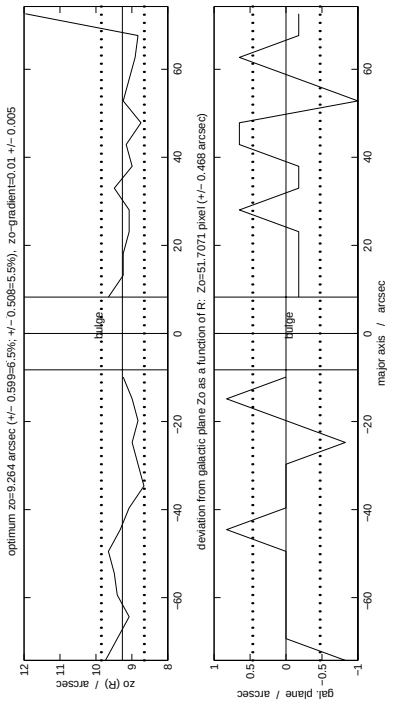

UGC 231

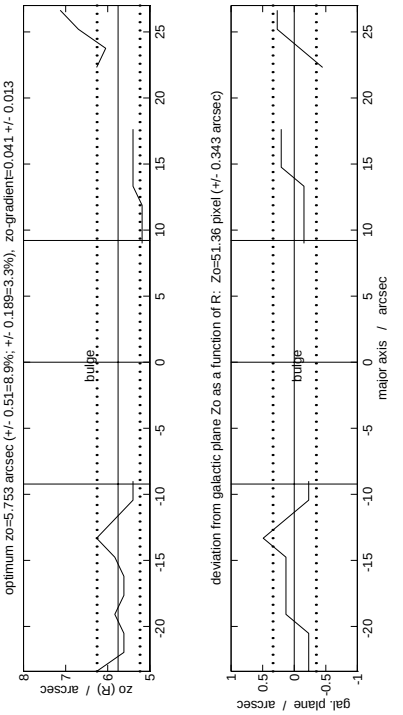

ESO 150-G07

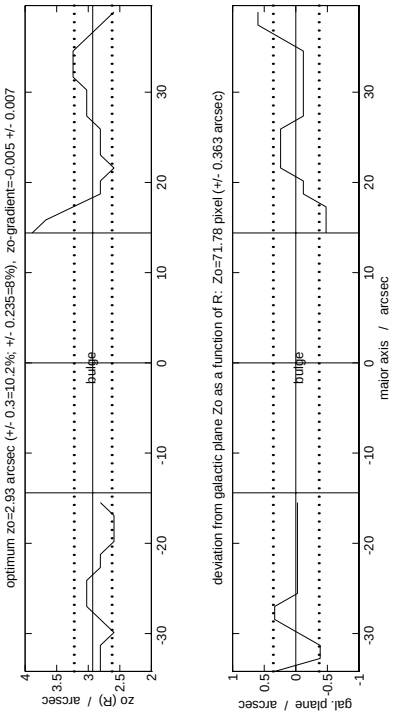

ESO 112-G04

Appendix B. The measured behaviour of scale height (upper panels) and mean galactic plane (lower panels) along the major axis of the disk, shown for each galaxy in the interacting/merging sample. The main output parameters are indicated. For details see Sect. 3 and Table 4 in this paper. Contour maps were given in Paper I, Figs. 4 and 5.

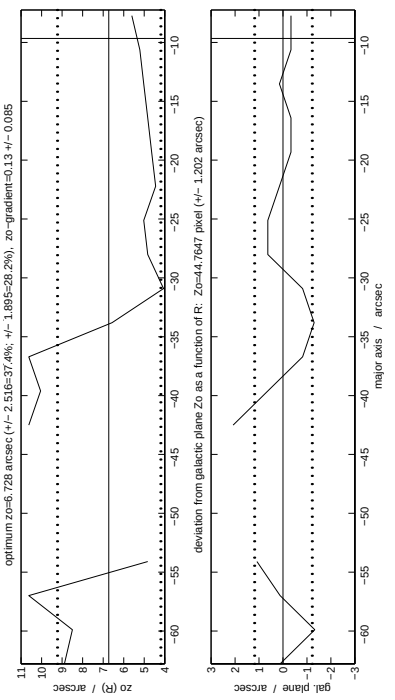

UGC 2411

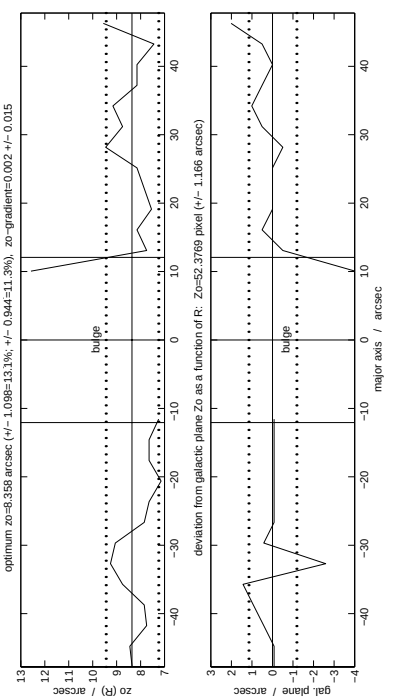

IC 1877

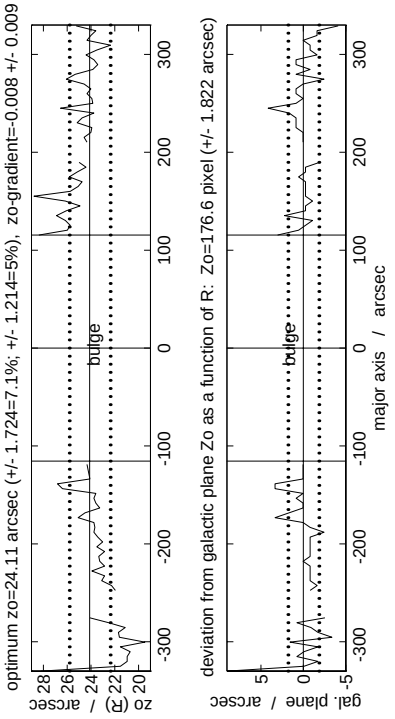

ESO 201-G22

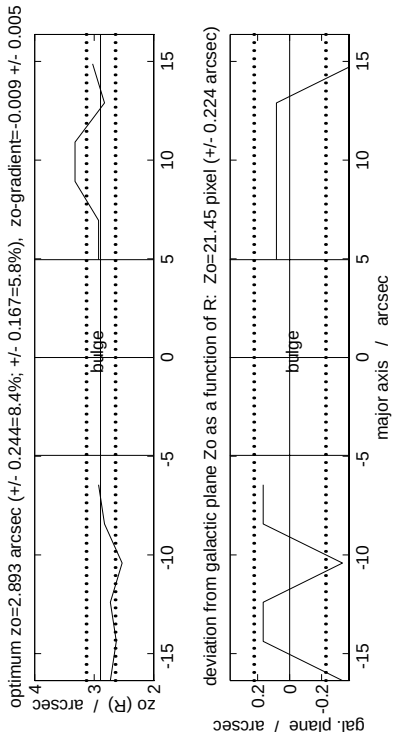

UGC 1839

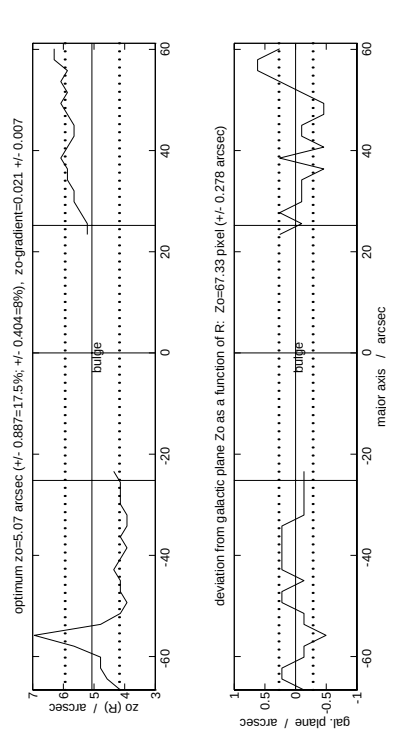

NGC 891

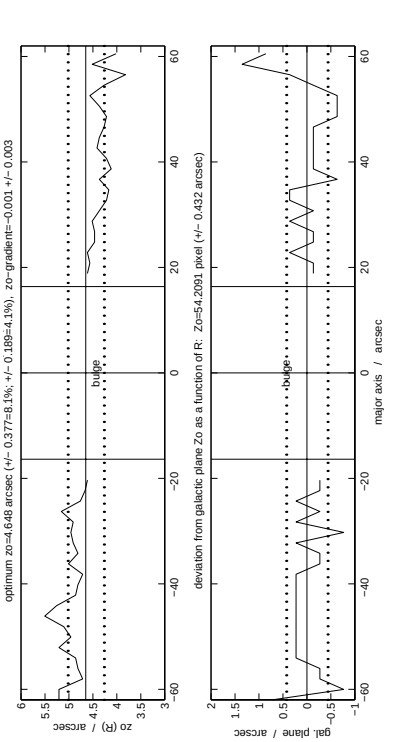

ESO 416-G25

Appendix B. (continued)

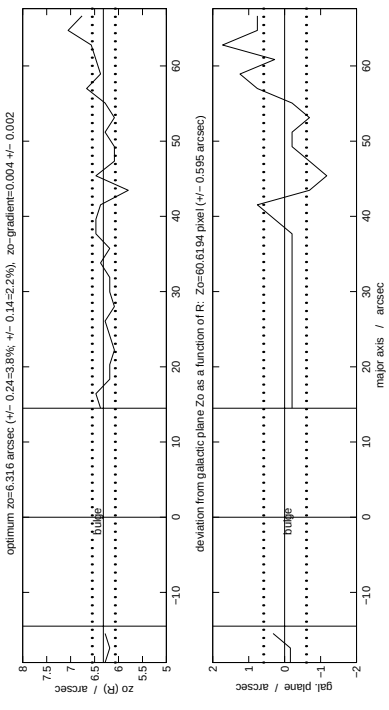

UGC 4278

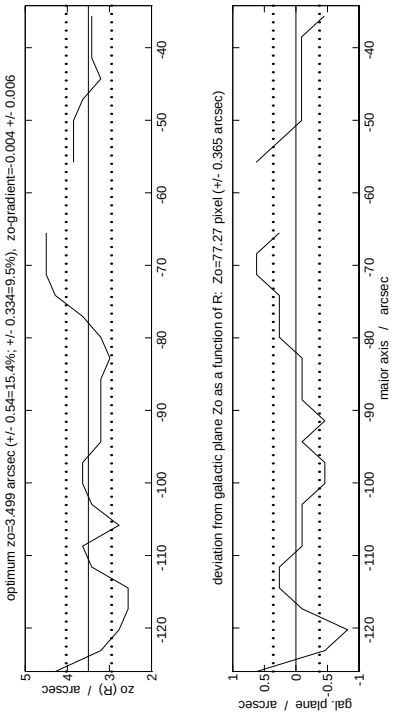

ESO 564-G27

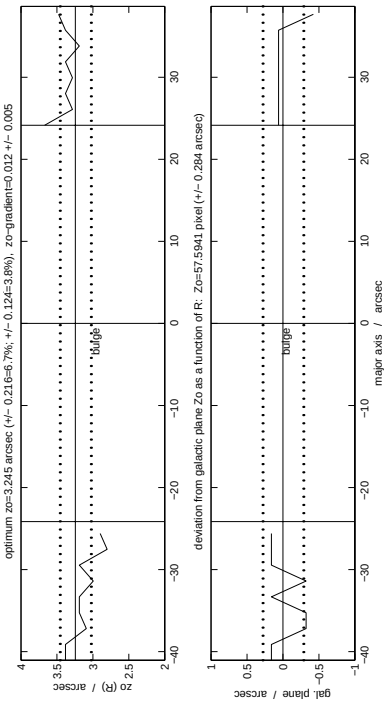

UGC 4943

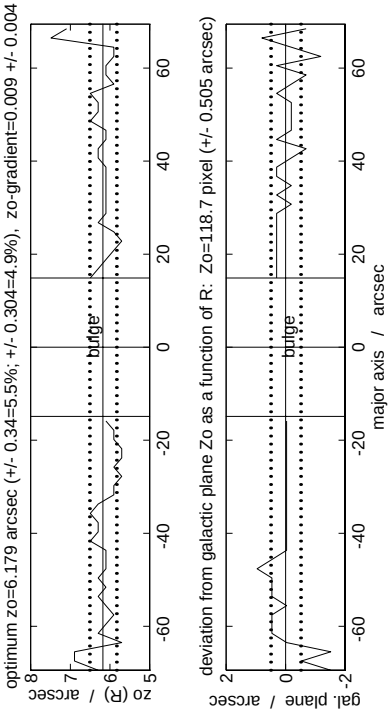

NGC 1886

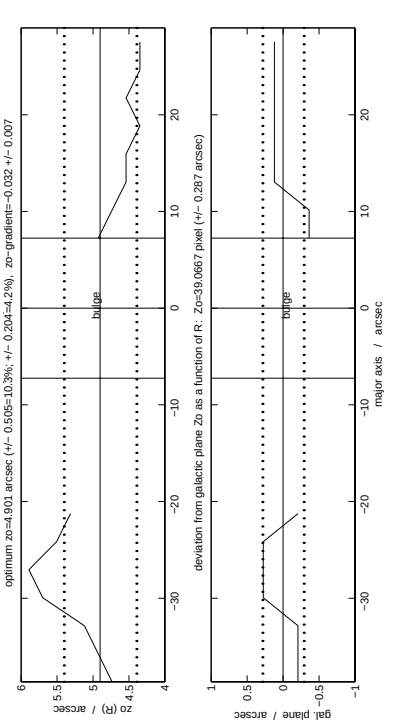

UGC 3474

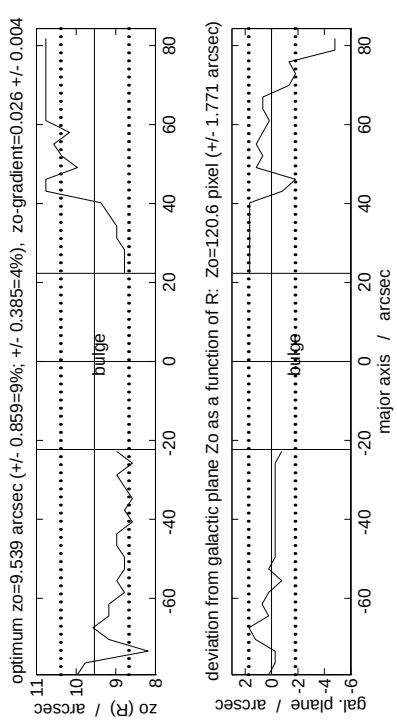

NGC 2310

Appendix B. (continued)

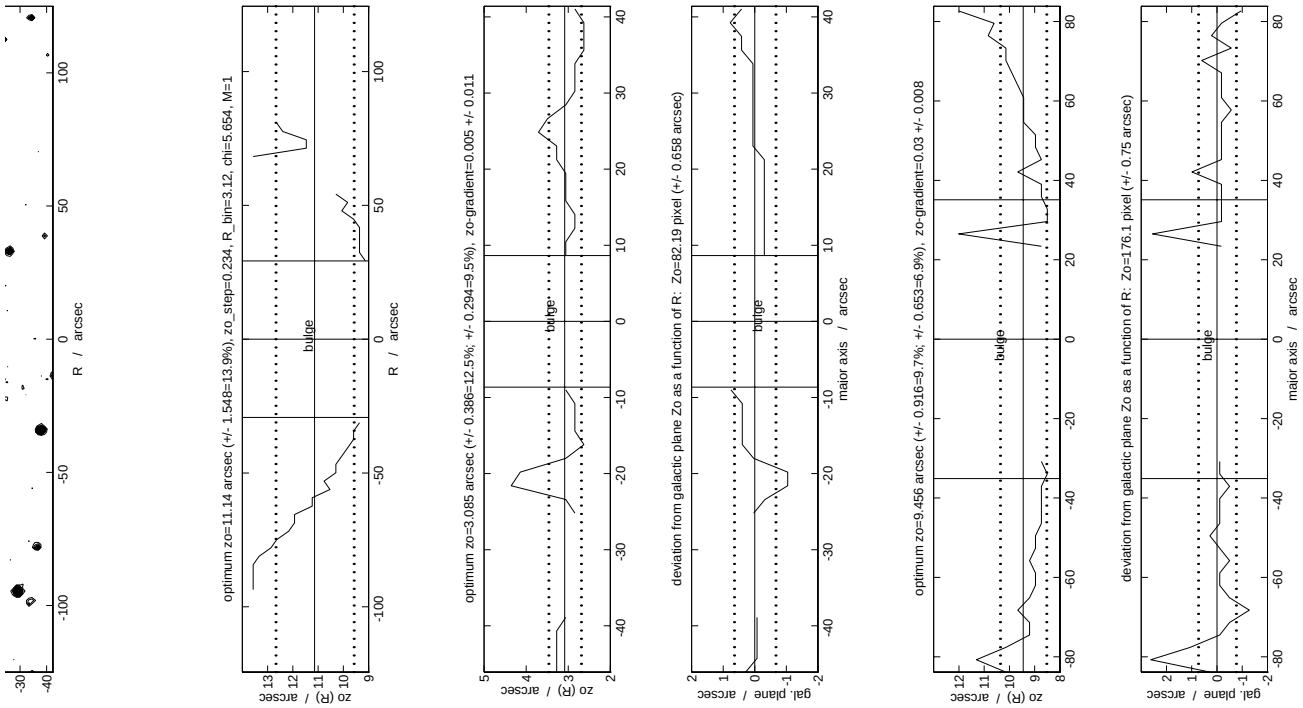

NGC 3390 ESO 319-G26 NGC 3957

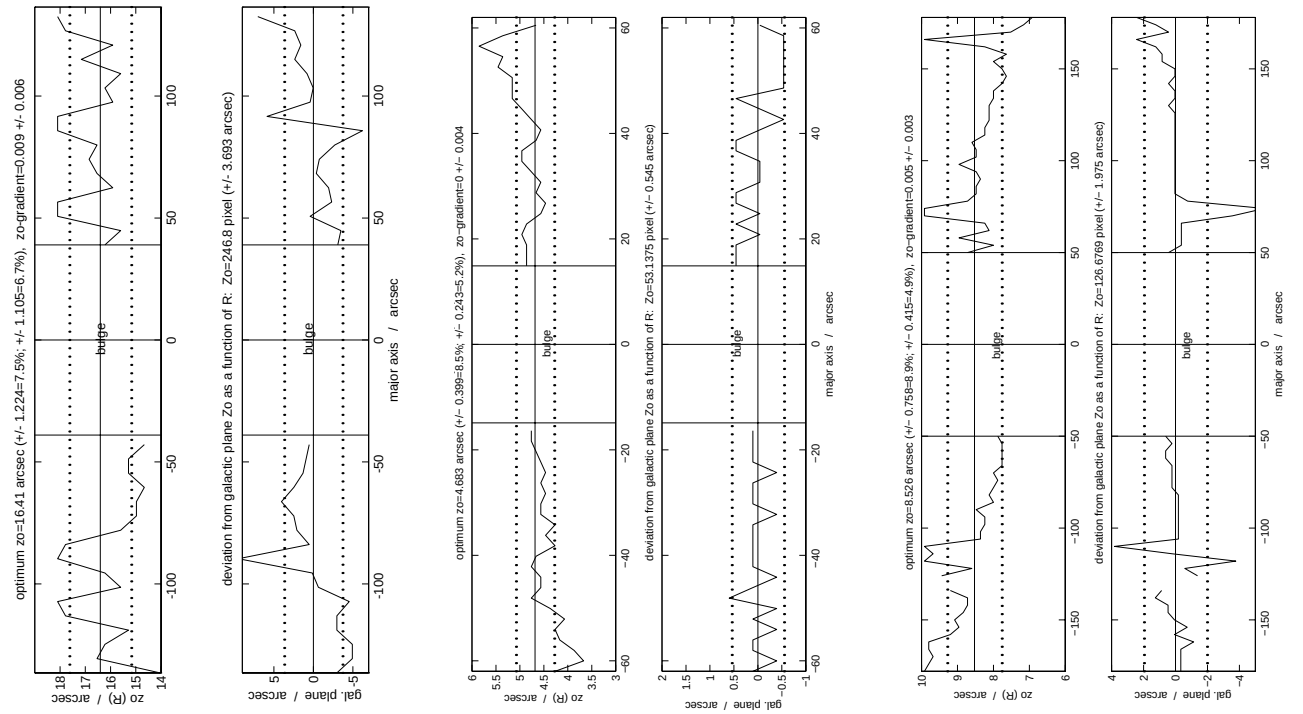

IC 2469 UGC 5341 IC 2531

Appendix B. (continued)

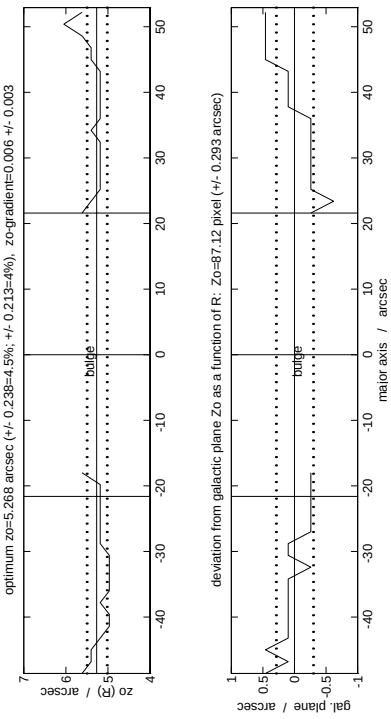

ESO 321-G10

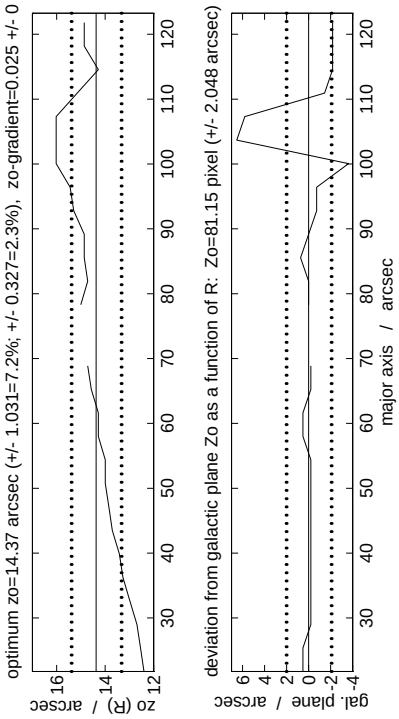

NGC 4217

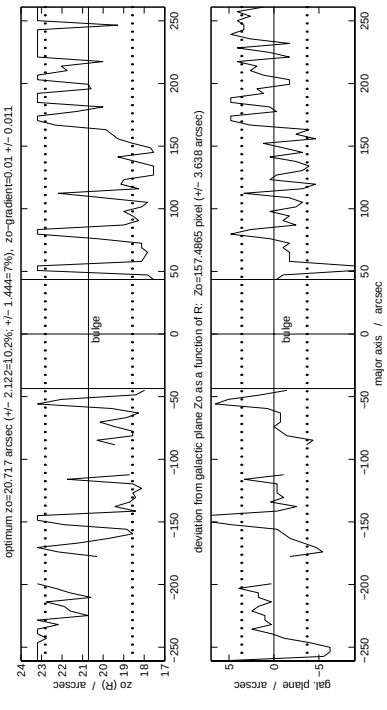

NGC 4244

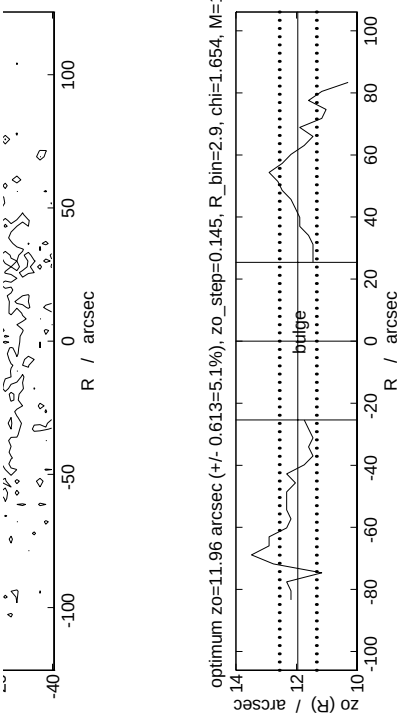

NGC 4013

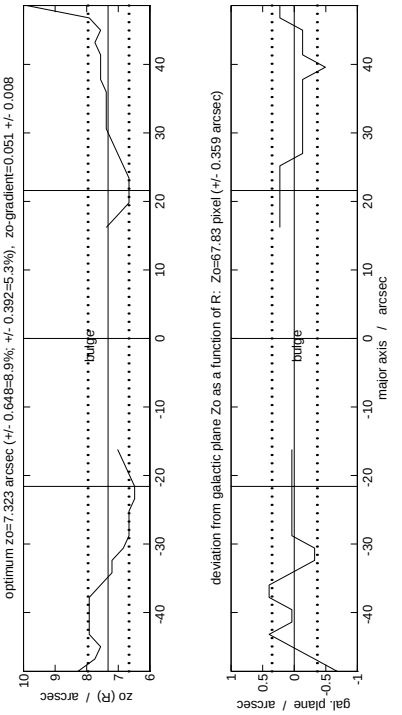

ESO 572-G44

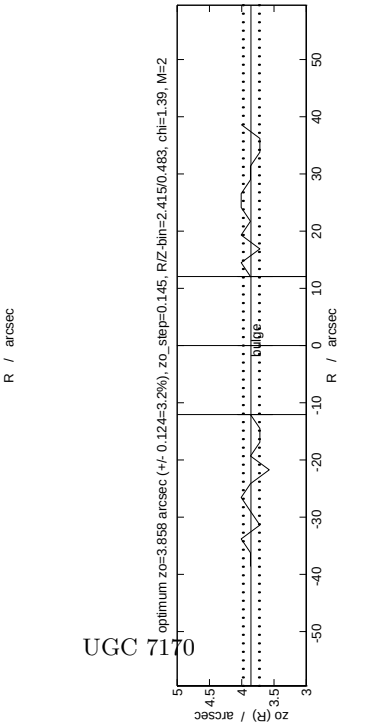

UGC 7170

Appendix B. (continued)

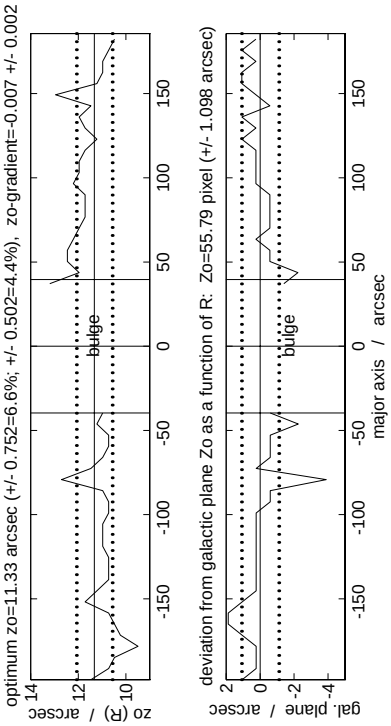

NGC 4565

NGC 4710

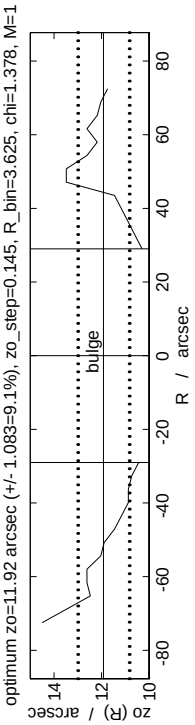

NGC 5170

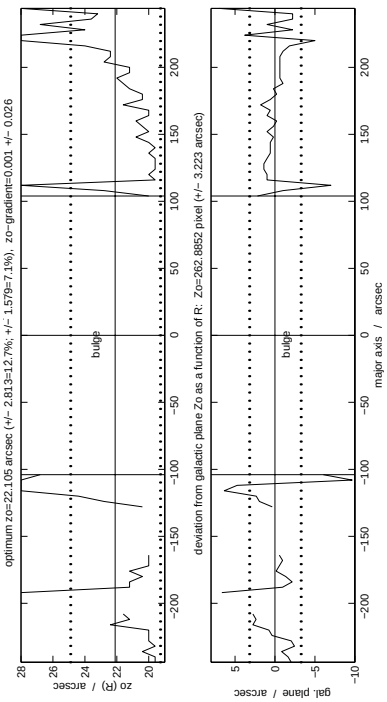

UGC 7321

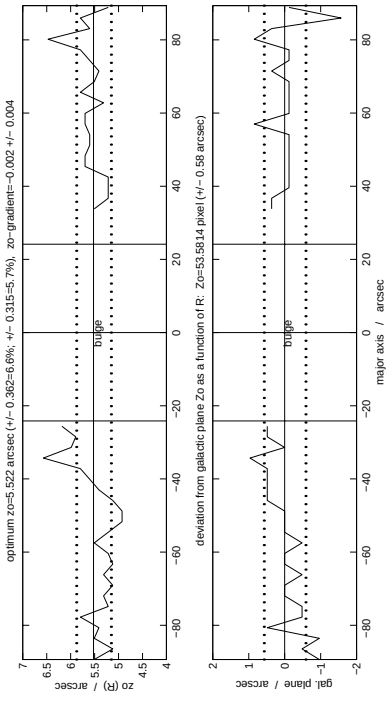

NGC 4302

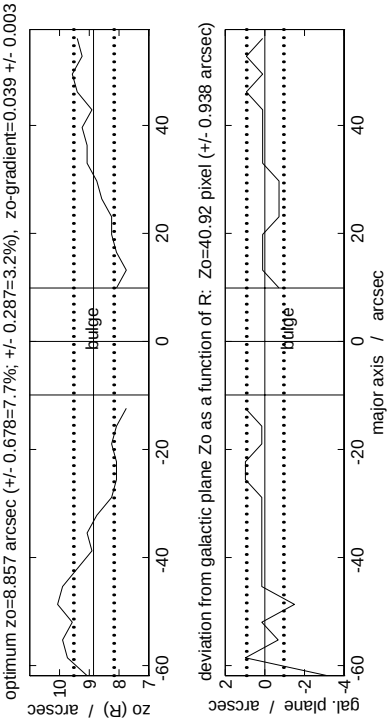

NGC 4330

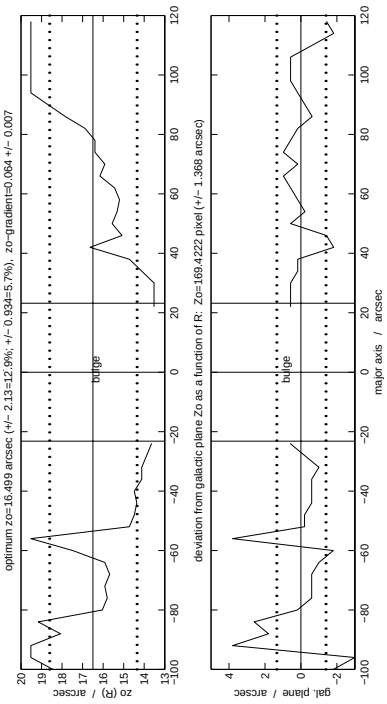

Appendix B. (continued)

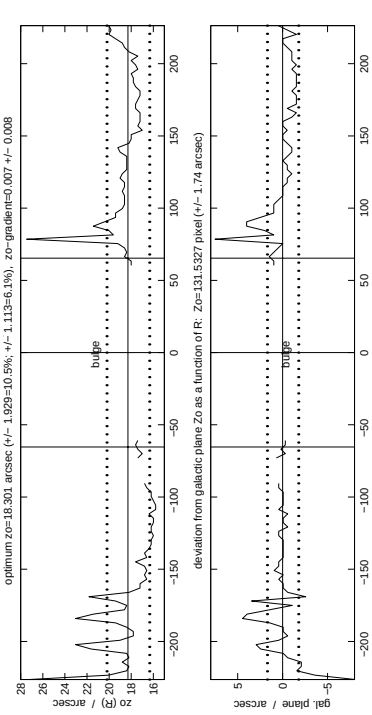

NGC 5907

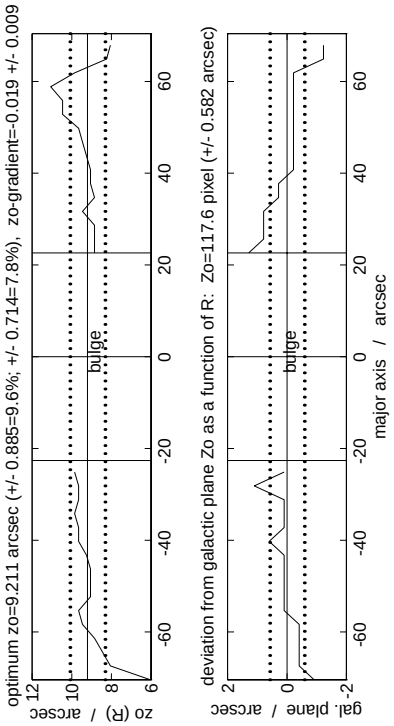

NGC 5908

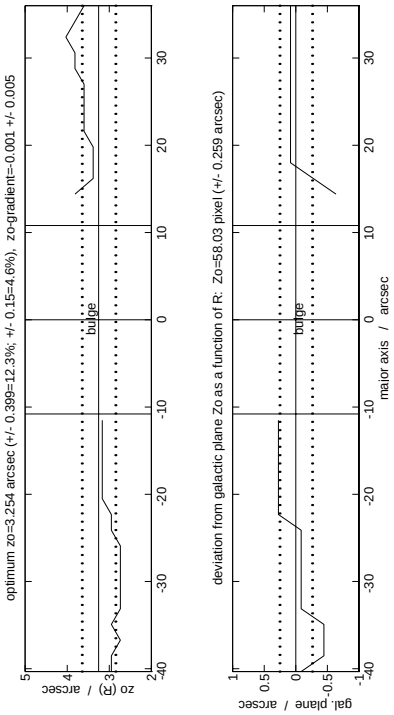

ESO 583-G08

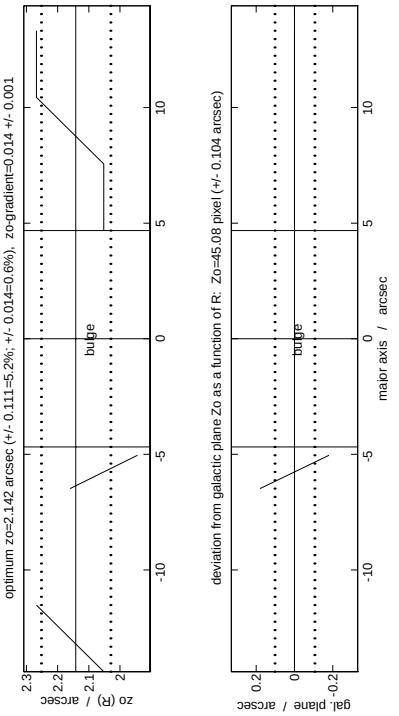

ESO 510-G18

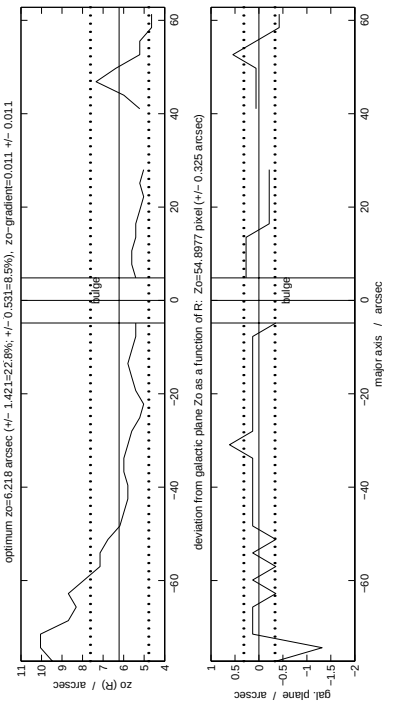

UGC 9242

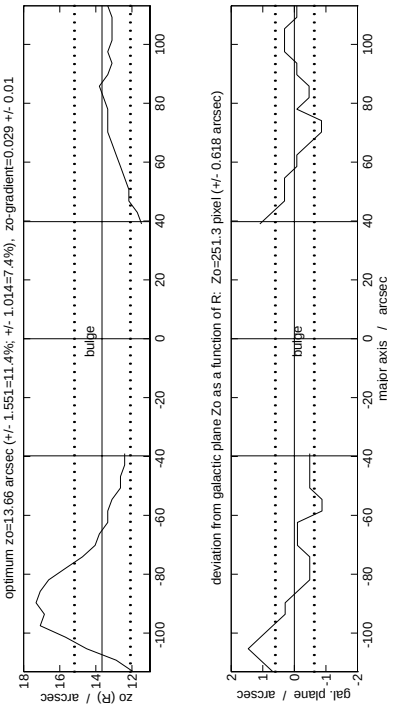

NGC 5775

Appendix B. (continued)

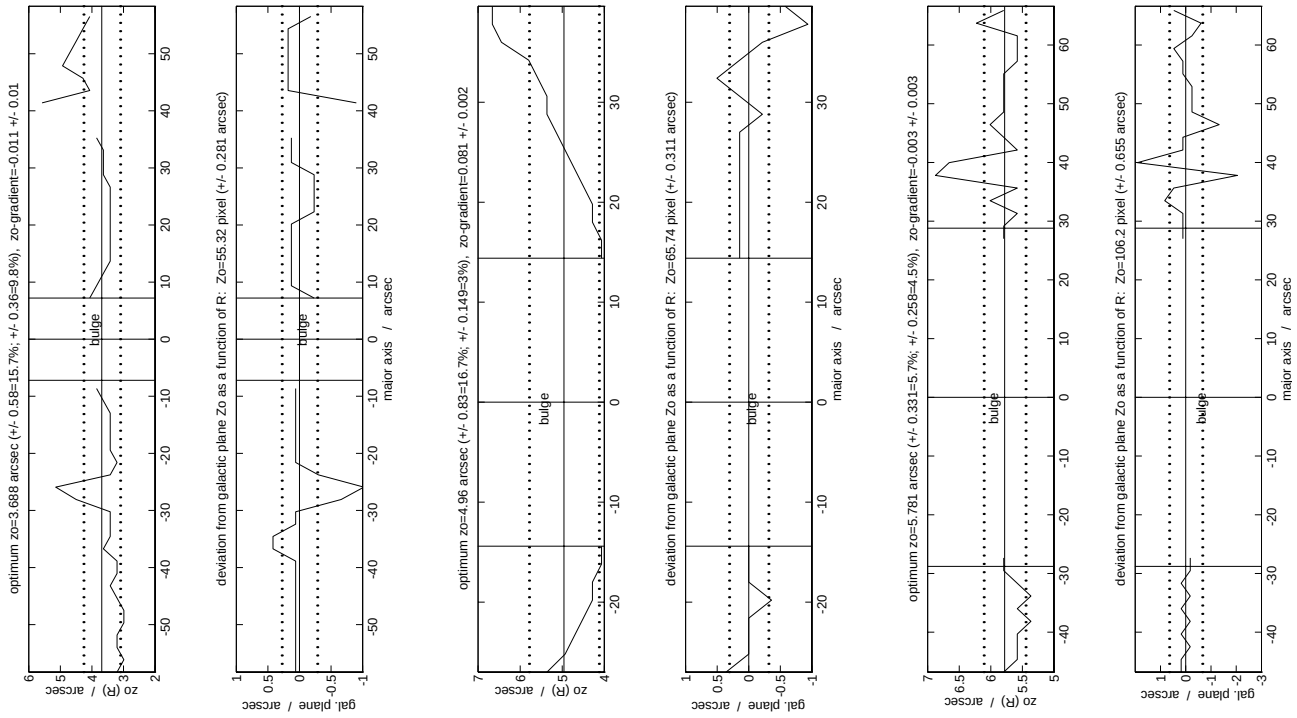

ESO 461-G06 ESO 339-G16 IC 4937

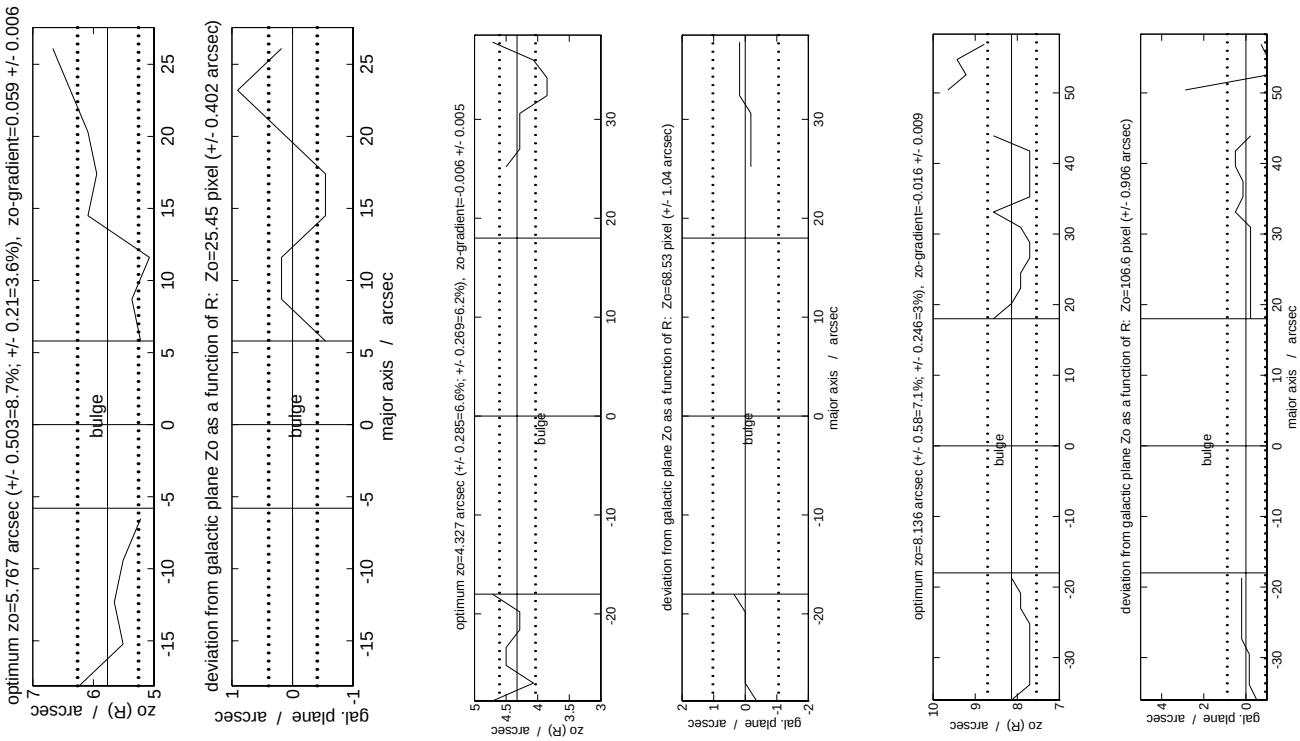

NGC 6181 ESO 230-G11 NGC 6722

Appendix B. (continued)

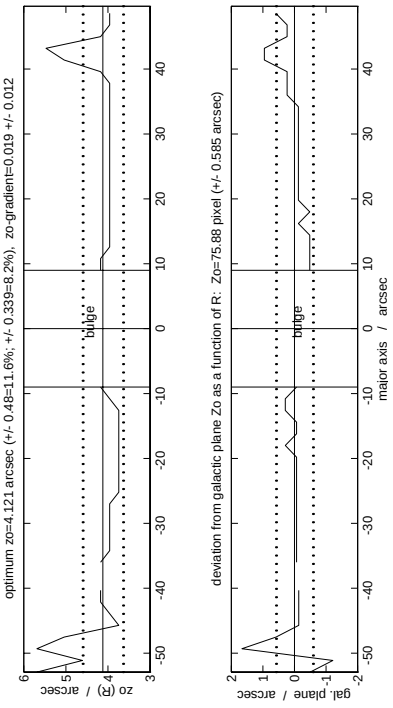

ESO 189-G12

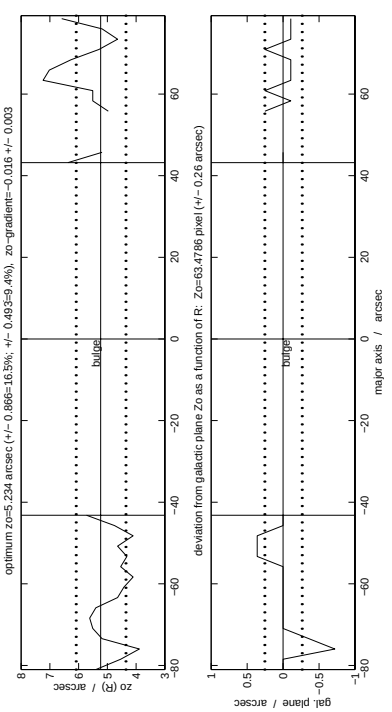

UGC 11859

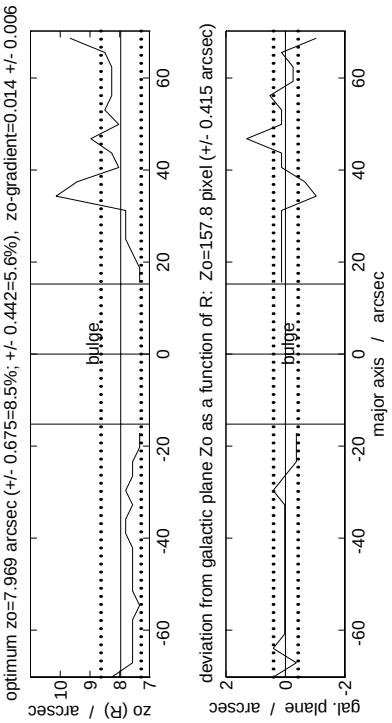

ESO 533-G04

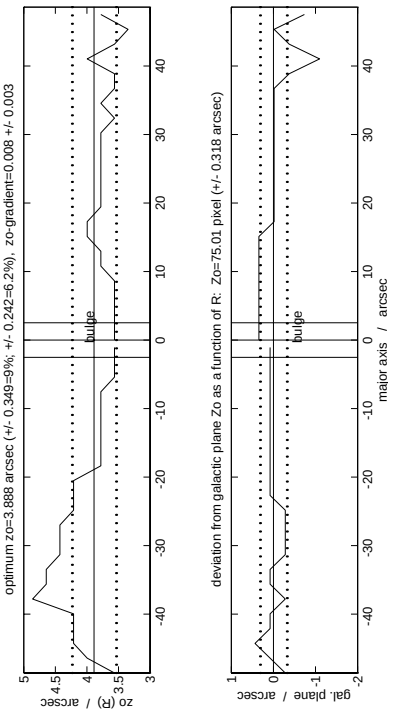

ESO 187-G08

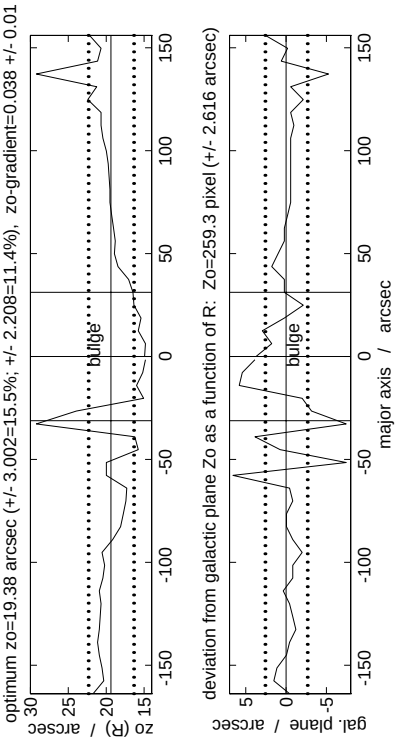

IC 5052

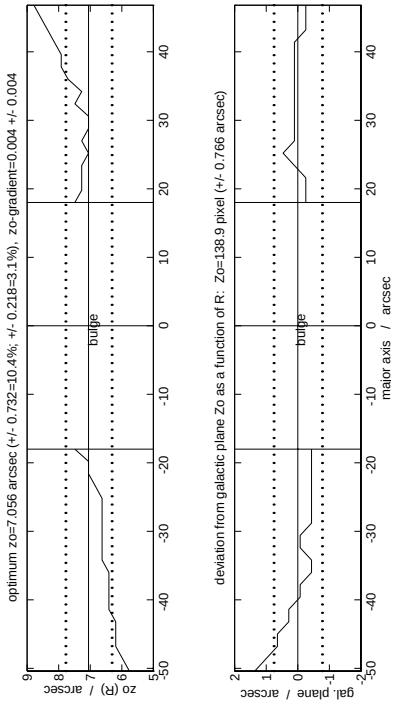

ESO 466-G01

Appendix B. (continued)

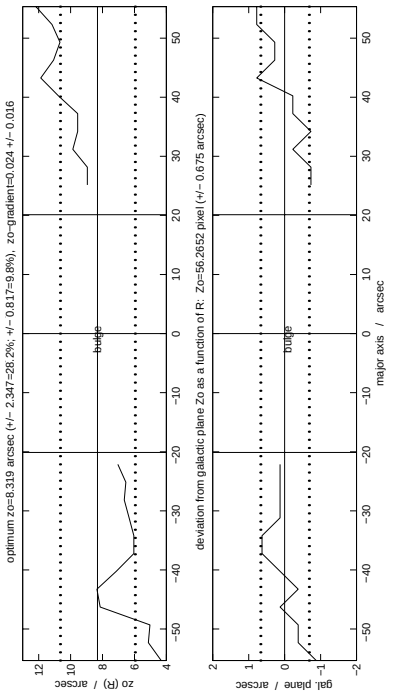

UGC 12423

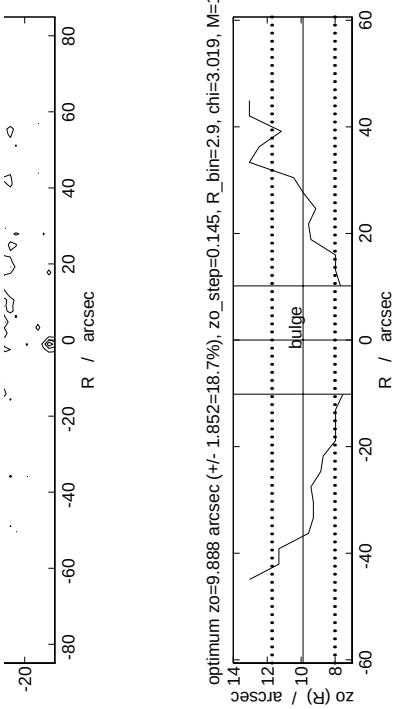

NGC 7518

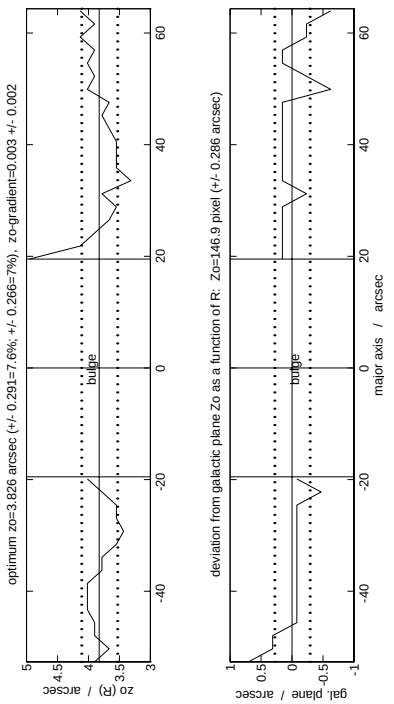

ESO 604-G06

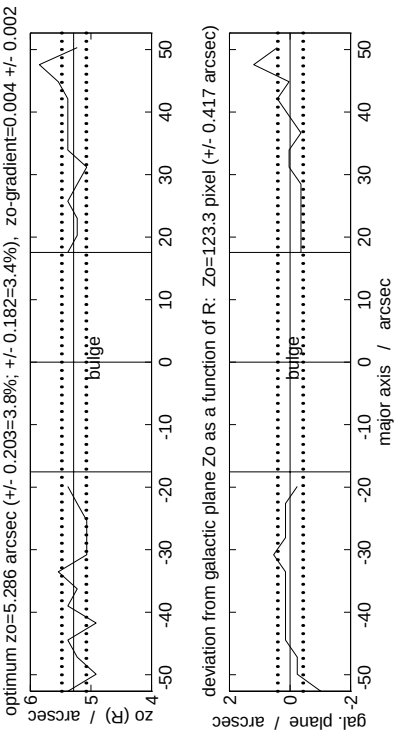

IC 5199

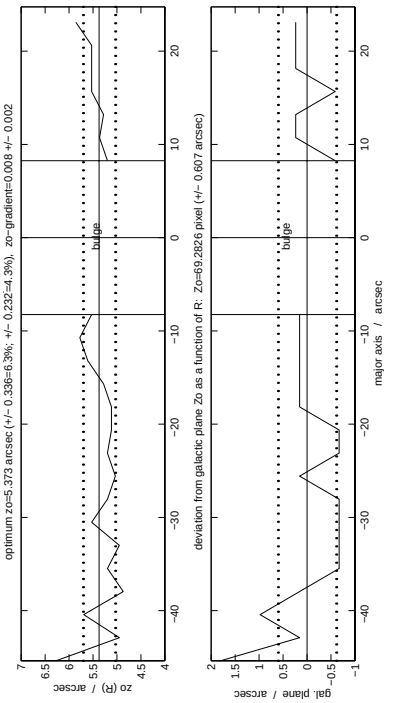

UGC 11994

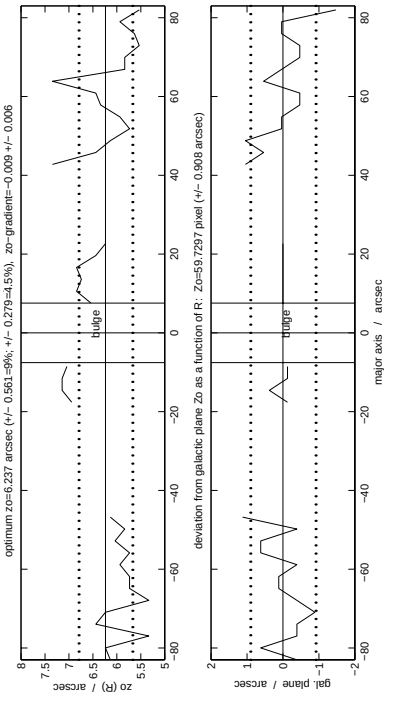

UGC 12281

Appendix B. (continued)